THESIS

SPATIAL ASYNCHRONY AND CROSS-SCALE CLIMATE INTERACTIONS IN POPULATIONS OF A COLDWATER STREAM FISH

Submitted by

George P. Valentine

Graduate Degree Program in Ecology

In partial fulfillment of the requirements

For the Degree of Master of Science

Colorado State University

Fort Collins, Colorado

Spring 2023

Master's Committee:

Advisor: Yoichiro Kanno
Co-Advisor: Mevin B. Hooten

Ryan R. Morrison

ABSTRACT

SPATIAL ASYNCHRONY AND CROSS-SCALE CLIMATE INTERACTIONS IN POPULATIONS OF A COLDWATER STREAM FISH

Climate change affects animal and plant populations over broad geographic ranges due to spatially autocorrelated abiotic conditions known as the "Moran Effect". However, populations do not always respond to broad-scale environmental changes synchronously across a landscape. We used a retrospective analysis of time-series count data (5-28 annual samples per site) at 170 stream segments dispersed over nearly 1,000 km to characterize the population structure and scale of spatial population synchrony in a coldwater stream fish (brook trout, *Salvelinus fontinalis*), which is sensitive to temperature and flow alterations, across its southern native range. Spatial synchrony differed by life stage and geographic region: it was stronger in the juvenile life stage than the adult life stage and in the northern sub-region than the southern sub-region. Spatial synchrony of trout populations extended to 100-150 km but was much weaker than that of climate variables such as temperature, stream flow, and precipitation. Early life stage abundance changed over time due to annual variation in summer temperature and winter and spring stream flow conditions. Climate effects on abundance differed between sub-regions and among local populations, indicating multiple cross-scale interactions where climate interacted with local habitat to generate only a modest pattern of population synchrony over space. Population synchrony was not spatially autocorrelated at the regional or sub-regional scales. We conclude that heterogeneous responses to climate variation lead to only a modest level of spatial synchrony among local trout populations, which leads to varying susceptibility to climate change. This response heterogeneity indicates that some local segments characterized by population asynchrony and resistance to climate variation could represent unique populations of this iconic native coldwater fish that warrant attention in their conservation

planning in a changing climate. Identifying such priority populations and incorporating them into landscape-level conservation planning is imperative to their conservation. Our approach is applicable to other widespread aquatic species sensitive to climate change.

Keywords: Bayesian, brook trout, climate, Portfolio Effect, stream fish, synchrony

ACKNOWLEDGEMENTS

We thank the numerous agencies and organizations that provided the data utilized in this study. Without the hard work of numerous biologists, technicians, and volunteers, this study would not have been possible. This research was funded by Cooperative Agreement No. G21AC10205 from the U.S. Geological Survey Southeast Climate Adaptation Science Center, and Cooperative Agreement No. F20AC11372 from the U.S. Fish and Wildlife Service. The findings and conclusions in this report are those of the authors and do not necessarily represent the views of the U.S. Fish and Wildlife Service.

TABLE OF CONTENTS

1 INTRODUCTION

Populations commonly experience shared temporal variation in abundance or demographic rates across a landscape. This spatial synchrony is often the strongest between nearby populations due to spatially autocorrelated abiotic conditions, known as the Moran Effect (Moran, 1953; Royama, 1992) and biotic processes such as movement and predation (Koenig, 1999; Liebhold et al., 2004; Ranta et al., 1995). Spatially homogeneous population responses have been reported for distances near 1,000 km in some animals and plants (Koenig & Knops, 1998; Post & Forchhammer, 2002; Ranta et al., 1997). Such broad-scale responses are attributed to continental and regional climate patterns, which are key drivers of demographic rates (Koenig, 2002; Stenseth et al., 2002). The shared spatial scale of synchrony between climate drivers and population responses is typically regarded as a sign of the Moran Effect (Koenig, 1999; Moran, 1953). As climate change accelerates, understanding the scale and drivers of spatial synchrony is critical to range-wide species conservation and management (Hansen et al., 2020).

Spatial synchrony as a result of climate is common in animals and plants, however local populations, even those in close geographical proximity, do not always display synchronous population trajectories (Herfindal et al., 2022; Sutcliffe et al., 1996). Heterogeneous population responses result not only because the magnitude of climate variation differs over space but also because the capacity to buffer against it differs locally. This cross-scale interaction between a broad-scale driver (e.g., climate) and local populations can occur due to the fine-scale spatial heterogeneity created by features such as local topography, microclimate variation, and surface-groundwater exchange (Fridley, 2009; McLaughlin et al., 2017). As a result, the strength of cross-scale interactions determines how synchronously a set of local populations respond to broad-scale drivers (Vendrametto Granzotti et al., 2022). A variety of asynchronous population trajectories buffers species from

range-wide declines (Heino et al., 1997; Roy et al., 2005), stabilizes populations over time at the regional scale (Portfolio Effect, Schindler et al., 2010; Schindler et al., 2015; Wilcox et al., 2017), and increases socioeconomic resilience of resource use (e.g., hunting and angling, Cline et al., 2022). However, little empirical knowledge exists about how synchronous and asynchronous populations are situated across the landscape in widely-distributed species.

Stream systems offer a unique opportunity for the study of macrosystems processes such as spatial synchrony and cross-scale interactions (McCluney et al., 2014). Streams are inherently characterized by spatial autocorrelation because environmental patterns and processes downstream are influenced by those upstream due to unidirectional flow (Isaak et al., 2017; Lloyd et al., 2005; Peterson et al., 2006). However, these processes are typically counteracted by spatial heterogeneity and network geometry created by stream confluences (Boddy et al., 2019; Frissell et al., 1986; Terui et al., 2018). Confluences represent geomorphic breaks where physical habitat characteristics such stream size, temperature, and channel slope change abruptly, creating spatial heterogeneity in abiotic conditions (Benda et al., 2004) and demographic responses (Childress et al., 2019) across stream networks. Consequently, stream habitat is often characterized and classified by segment (i.e., from confluence to confluence, Frissell et al., 1986; U.S. Geological Survey, 2016). The stream segment is also the finest spatial grain at which stream habitat data are available at the national and continental scale (e.g., National Hydrography Dataset Plus (NHDPlus) data set in the USA). Stream confluences are more numerous and average segment length is shorter in headwaters than farther downstream in stream networks (Wohl, 2017). Therefore, headwater stream networks contain habitat heterogeneity over relatively short physical distances, providing a template on which cross-scale interactions can occur.

Globally, headwater streams harbor a significant portion of remaining populations of cold-water fish such as trout and salmon, which are sensitive to variation in stream temperature and flow

(Kovach et al., 2016). Temperature and flow are key abiotic drivers of population and community dynamics in stream biota (Maheu et al., 2016; Poff et al., 1997). Atmospheric air temperature, a key influence on and common surrogate for stream temperature, has increased dramatically in the last century and is predicted to further increase (Pörtner et al., 2022). In the southeast USA, climate change is projected to increase precipitation and the occurrence of extreme flood events (Alipour et al., 2020; Ingram et al., 2013). Stream salmonids respond to both high temperatures and high extremes of streamflow (Goode et al., 2013; Kanno et al., 2017; McCullough et al., 2009; Santiago et al., 2017). Climate effects on stream fish also vary by life stage and season. Early life stages of fish are particularly sensitive to changes in streamflow: Stable summer and fall stream flow results in increased growth and abundance, but scouring winter flows during incubation and emergence can wash away eggs and newly hatched individuals (Cattanéo et al., 2002; Kanno et al., 2015; Kovach et al., 2016; Schlosser, 1985). As stronger swimmers, adults are less sensitive to high streamflows, however high water temperatures can result in increased stress and direct mortality, as well as impact the timing of spawning (Kovach et al., 2016; Warren et al., 2012). As climate change amplifies the above effects, stream fish populations at the rear margins of their ranges are particularly vulnerable (Hampe & Petit, 2005; Pregler et al., 2018).

We characterized the climate drivers of spatial synchrony by life stage (i.e., juvenile and adult) among populations of an iconic native coldwater fish (brook trout, *Salvelinus fontinalis*) across multiple spatial scales in the southern portion of their native range in the eastern USA. Remnant populations of this salmonid in the study region occur in small, isolated headwaters (Kazyak et al., 2022), which limit potential for dispersal among populations. Furthermore, predation impacts from other species are low as many populations occur in allopatry (Hudy et al., 2008), precluding dispersal and predation as factors that might otherwise synchronize population trajectories over space. Brook trout are highly sensitive to climate drivers such as stream temperature and

flow (Kanno et al., 2017; Roghair et al., 2002; Warren et al., 2012; Xu et al., 2010). Consequently, this species provides an opportunity to investigate population synchrony attributable mainly to climate variation.

Our study aims were threefold. First, we quantified the scale and strength of spatial synchrony among brook trout populations and compared it with those of spatial synchrony in climate variables (i.e., temperature, precipitation, and streamflow). We hypothesized that patterns of spatial synchrony would be similar between the climate variables and trout populations, if climate variables exerted a strong and spatially homogeneous effect on population trajectories (Koenig, 1999; Levin, 1992; Wiens, 1989). Second, we tested whether spatial synchrony was explained by a set of seasonal climate variables and whether the importance of seasonal climate variables differed between and within northern and southern sub-regions. Because we studied a sensitive coldwater species at its southern range limit, we predicted that temperature would be a stronger driver of synchrony in southern populations compared to northern populations (Maitland & Latzka, 2022). Furthermore, we predicted that stream flow would be a stronger driver of synchrony in the young-of-the-year (juvenile) stage versus adult stage due to the diminished ability to withstand bed-scouring high flows of the younger stage (Kanno et al., 2016; Kovach et al., 2016). Third, we quantified stream segment-specific population trajectories relative to the overall trajectory across segments to characterize how synchronous and asynchronous populations are distributed in the landscape. Asynchronous populations that deviate from the overall trajectory hold conservation value when asynchrony is due to population resiliency to environmental changes or habitat serving as climate refuge (Hilborn et al., 2003; Schindler et al., 2010; Schindler et al., 2015). To address these aims, we assembled time-series abundance data at 170 stream segments spanning nearly 1,000 km of brook trout habitat across the southern Appalachian mountains of eastern North America.

2 METHODS

2.1 Study Species

Brook trout are native to eastern North America, distributed from the Appalachian Mountains in northern Georgia to the coasts of Newfoundland and Labrador. They are culturally and economically important, designated as the state fish of nine US states. Brook trout are among the most popular freshwater sportfish in the US (American Sportfishing Association & Sport Fish Restoration, 2021). They spawn in fall, and their eggs overwinter in streambed nests ("redds") to hatch in early spring (Hazzard, 1932). They can reach maturity as early as one year of age, and seldom live longer than 3 years in their southern range (Donald & Alger, 1989; Larson & Moore, 1985; Meyer et al., 2006). Brook trout are highly sensitive to water temperature and cannot withstand prolonged temperatures above 22-24°C (Eaton et al., 1995; Wehrly et al., 2007) and spawning is deleteriously affected by high summer and fall temperatures (Warren et al., 2012). Redds are scoured and young brook trout are swept away by high stream flows during winter and spring months (Kanno et al., 2015). Because of their high environmental specificity, brook trout are often considered to be an aquatic indicator species. Due to anthropogenic activities, they have experienced large declines, particularly in their southern native range (Hudy et al., 2008).

Evidence suggests that if spatial synchrony occurs in brook trout, it is likely due to the Moran Effect rather than dispersal dynamics because stream populations typically are isolated by unsuitable riverine habitats. Kanno et al. (2016) found that seasonal air temperature and precipitation led to spatial synchrony in young-of-the-year (YOY) brook trout, but not in adults. Zorn & Nuhfer (2007) found correlations between brook trout density and spring discharge in Michigan rivers. Spatial synchrony due to the Moran Effect has been described in other stream-dwelling salmonids such as brown trout (*Salmo trutta*, Cattanéo et al., 2003; Lobón-Cerviá, 2007;

Zorn & Nuhfer, 2007). Despite these indications of synchrony in brook trout, prior work has been limited to single datasets (i.e., Kanno et al., 2016; Zorn & Nuhfer, 2007), and no study has attempted a broad-scale analysis of spatial synchrony in this species.

2.2 Study Area and Dataset

Our study area comprised the far southern and eastern native range of brook trout in the USA, from the southern Appalachian Mountains in Georgia to Maryland (Fig. 1). We compiled a dataset with over 200,000 brook trout individuals in 170 stream segments from nine state, federal, and private sources between 1982 and 2015 (Table S1). All segments had ≥ 5 years of data during this time period. Conserved areas such as Great Smoky Mountains National Park, Shenandoah National Park, and several long-term study segments had richer spatial and temporal coverage. Data consisted of individual trout measurements, sampling occasion data, and stream segment data. Individual trout measurements included total length (mm) and weight (g). Sample data included date and number of electrofishing passes. Stream segment data included National Hydrography Dataset Plus (NHDPlus) stream segment common identifier (COMID), coordinates (decimal degrees), elevation (m), length and median width (m). Study segments were located in headwater streams with a mean wetted width of 5.1 m (Table 1). We divided the northern and southern sub-regions at 37.13° latitude – that of the New River Valley, which aligns with a major shift in genetic patterns of this species (Kazyak et al., 2022). The mean elevation was higher and channel slope was steeper in the southern versus northern sub-region (906 m versus 462 m in elevation; 6.6% versus 3.6% in slope). The mean maximum summer air temperature was higher in the southern sub-region (25.7°C) than in the northern sub-region (24.6°C).

All brook trout data were collected by backpack electrofishing in wadeable streams (mean site length: 128m). A combination of single- and multi-pass sampling methods (single: 29.9%,

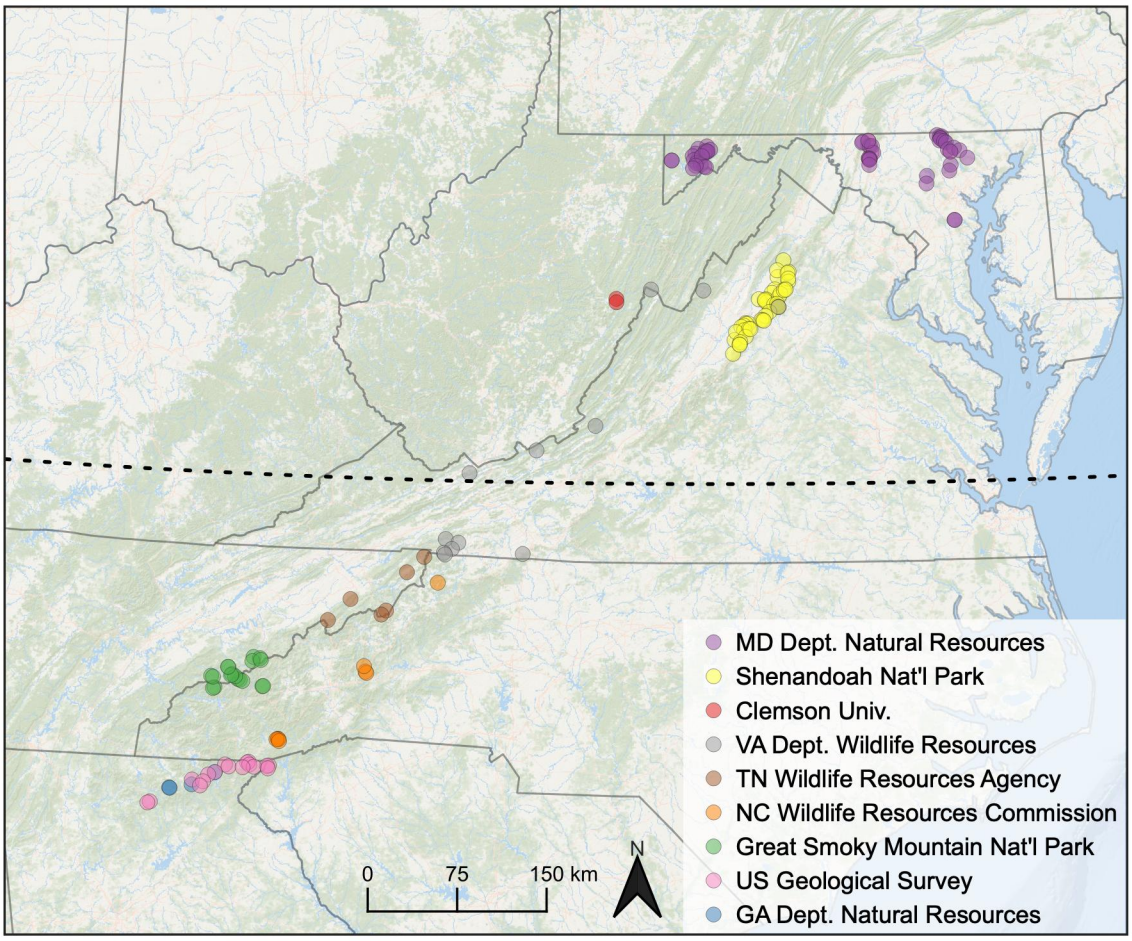

Figure 1: Map of 170 study stream segments where electrofishing data were available (5-28 annual samples per segment). Dotted line (37.13° latitude) divides north and south sub-regions. Dot colors represent the agencies/groups that collected the data. MD = Maryland, VA = Virginia, TN = Tennessee, NC = North Carolina, GA = Georgia. Basemap: ESRI.

Table 1: Summary statistics for segment characteristics and climate variables (1980-2015) by sub-region. Summer: June-Sep. Winter: Dec. - Feb. Spring: Mar. - May. Sources: ORNL DAYMET, USGS NHDPlus.

	North		South	
	Mean	SD	Mean	SD
Channel Slope (%)	3.6	2.9	6.6	4.7
Length (km)	3.7	2.9	2.8	1.7
Catchment area (km^2)	6.9	9.1	3.6	3.1
Elevation (m)	461.9	212.4	905.5	207.7
Stream order	2.0	1.0	1.0	1.0
Wetted width (m)	5.1	3.1	5.1	2.4
Max Summer Temperature (C)	24.6	2.5	25.7	1.8
Max 0.9Q Winter Stream Flow (CFS)	61.2	225.8	56.9	143.8
Max 0.9Q Spring Stream Flow (CFS)	104.4	368.5	55.9	134.6

multi: 70.1%) was employed following standardized sampling protocols for the southern US region (SDAFS Trout Committee, 1992). In multi-pass sampling, fish were removed from the stream in successive passes in temporarily blocked stream reaches to estimate capture probability and thus population size. Sampling boundaries were defined by block nets or cobble dams which serve as barriers for fish movement. Depending on stream width, one to three backpack electrofishing units were used. A majority of sampling occurred in annual surveys conducted at the same sites in June - October. Samples taken in lakes and ponds, as well as observations of hatchery-born fish, were excluded. We also excluded segments with less than 10% brook trout in fish assemblages. YOY brook trout were defined as those <= 90 mm total length, and adults were defined as those >90 mm total length. We summarized the data to counts by life stage, sampling occasion, and electrofishing pass.

To spatially match trout data with predictors, we pooled trout count and surface area surveyed across sites when multiple sites were surveyed annually in an NHDPlus stream segment (a length of a stream delineated by either its beginning and a confluence, or by two confluences (U.S. Geological Survey, 2016); average segment length = 3.3 km). Brook trout in headwaters typically remain within several hundred meters of their hatching locations (Hudy et al., 2010; Rodríguez, 2002). Thus, pooling count data by stream segment allowed us to account for dispersal and demographic dependence within segments. On average, 34% of stream segments contained more than one collection site.

2.3 Correlogram Analysis

We quantified the magnitude and scale of spatial synchrony in YOY and adult brook trout using the nonparametric spatial covariance function in the 'ncf' package for R (Bjornstad, 2022; Bjørnstad & Falck, 2001; R Core Team, 2022). We then extracted estimates of both initial and average spatial

correlation and the (Euclidean) distances to which spatial covariance extends. We visually represented synchrony using spline correlograms, which portray the spatial decay in pairwise correlation between segments. The scale of synchrony (correlation length) can be interpreted as the distance at which the confidence envelope of the spline function is significantly higher than the sample average (x-axis, Bjørnstad & Falck, 2001). We selected 72 stream segments with 5 years or more multi-pass electrofishing data between 1995 and 2015. We further removed segments where the focal life stage was never collected, resulting in 66 segments for YOY and 68 segments for adults. We conducted the correlogram analysis of the two life stages at both the regional and sub-regional levels. We calculated 95% confidence intervals for the correlograms using the bootstrap algorithm in the 'ncf' package. We truncated pairwise (Euclidean) lag distances to 2/3 the total distance observed following Fletcher et al. (2018). Abundances at each sample were predicted using the 'FSA' package for R (Ogle et al., 2022), which uses electrofishing depletion counts to estimate abundance. Using these predicted abundances, we calculated the natural log of average density (fish/1000 m^2) at each stream segment and year. We imputed missing data when necessary for the analyses and show in Appendix 4 that the results were insensitive to this imputation.

We compared the magnitude and scale of spatial synchrony in brook trout to mean summer water and air temperature and winter streamflow and precipitation (Kanno et al., 2015; Kanno et al., 2016). Observed air and water temperatures were obtained at 30-minute intervals from the USDA Forest Service (Li et al., 2016). These were measured using a network of 204 paired temperature loggers located in brook trout streams in the southeast US from 2011 to 2015 (Fig. S2). We summarized these temperatures to annual summer (June - September) means. Monthly streamflow estimates were obtained from the NHDPlus V2 (U.S. Geological Survey, 2016) for the stream segments used in the correlogram analysis of trout populations. We summarized these estimates to annual winter (December - February) means. Hourly observed winter precipitation (2008

- 2014) data were obtained for 51 NOAA NCEI measurement sites within the geographic extent of the trout data (Fig. S2, National Oceanic and Atmospheric Administration, National Centers for Environmental Information, 2022) and summarized to annual winter (December - February) totals.

2.4 Hierarchical Model

We developed two Bayesian hierarchical models to infer synchrony in brook trout populations and to identify climate drivers of synchronous dynamics (Berliner, 1996; Wikle et al., 1998). For both, we developed an N-mixture model (Royle, 2004) using a removal mechanism coupled with a log linear process model. In the first, hereafter the random effects model, we inferred brook trout count as a function of a temporal random effect and a spatiotemporal random effect. In the second, hereafter the climate effects model, we inferred brook trout count as a function of summer temperature and winter and spring streamflow. We elected to use separate models for climate and random effects after encountering convergence issues using a single, combined model (however the simulation in Appendix 4 demonstrates that parameters are identifiable in such a model). We analyzed counts of brook trout abundance from 170 stream segments collected between 1982 and 2015.

Adapting the standard N-mixture model to allow our removal sampling data at segment $i = 1, ..., n$, and year $t = 1, ..., T$ for each of $j = 1, ..., 3$ electrofishing passes, we specified the data model

$$y_{i,j,t} \sim \begin{cases} \text{binomial}(N_{i,t}, p_s) & \text{if } j = 1 \\ \text{binomial}(N_{i,t} - \sum_1^{j-1} y_{i,j,t}, p_s) & \text{if } j > 1\,, \end{cases} \tag{1}$$

where $y_{i,j,t}$ is observed count of YOY or adult brook trout at segment i, pass j, and year t. We denote $N_{i,t}$ as the predicted count of the given life stage in year t at segment i. We modeled abundance

separately for passes $j > 1$ because there are $\sum_1^{j-1} y_{i,j,t}$ fewer individuals in the sampling area after removing them in each pass. The term p_s represents the capture probability (of individuals) for data source $s = 1, ..., S$. We used informed priors for $\boldsymbol{p}$ such that $\boldsymbol{p} \sim \text{beta}(0.5, 0.1)$ for YOY and $\boldsymbol{p} \sim \text{beta}(0.65, 0.1)$ for adults, based on their differences in capture probability (Kanno et al., 2015). We allowed capture probability to vary by source because sampling crew measurement is often a large source of variation in sampling efficiency (Hughes et al., 2002; Kimmel & Argent, 2006; Meador, 2005). We modeled abundance in each stream segment and year conditional on local density $\lambda_{i,t}$ (fish/1000 m^2) as

$$N_{i,t} \sim \text{Poisson}\left(\frac{a_{i,t}}{1000}\lambda_{i,t}\right), \tag{2}$$

where $a_{i,t}$ is the sum of site areas (length $*$ median wetted width) sampled for stream segment i and year t.

For the climate effects model, local abundance was represented as a function of three climate covariates. Daily maximum air temperature predictions for each stream segment were obtained from the DAYMET model (Thornton et al., 1997, 2021; Thornton et al., 2014) using the 'daymetr' package in R (Hufkens et al., 2018). Monthly flow percentile predictions for each stream segment were obtained from the NHDPlus V2 (U.S. Geological Survey, 2016). We summarized summer high temperature as the mean of daily maximum predictions between June and September in year t - 1. We used previous year summer temperatures to account for temporal discrepancies between trout sampling and temperature measurements. We summarized winter (December - February) and spring (March - May) high stream flows as the maximum of monthly 90th percentile flow estimates. All climate covariates were centered and scaled by stream segment. Brook trout density was modeled as a function of these covariates $\boldsymbol{x}_{i,t}$ using the log-link function

$$\log(\lambda_{i,t}) = \omega_i + \boldsymbol{x}'_{i,t}\boldsymbol{\beta}_i, \tag{3}$$

where ω_i represents average log density at segment i when climate variables are set at their mean and $\boldsymbol{\beta}_i$ represents a vector of segment-specific climate covariate effects. Priors on ω_i and $\boldsymbol{\beta}_i$ were noninformative: $\omega_i \sim \text{normal}(0, 1000)$ and $\boldsymbol{\beta}_i \sim \text{normal}(\boldsymbol{\mu}_\beta, \boldsymbol{\sigma}^2_\beta)$ where $\boldsymbol{\mu}_\beta \sim \text{normal}(0, 100)$ and $\boldsymbol{\sigma}_\beta \sim \text{uniform}(0, 10)$. As a random effect, $\boldsymbol{\beta}_i$ allows the estimation of both local and overall covariate effects.

For the random effects model, local abundance was represented as a function of segment-specific intercept and two random effects:

$$\log(\lambda_{i,t}) = \omega_i + \epsilon_t + \gamma_{i,t}\,. \tag{4}$$

Where ω_i represents average log density at segment i with the diffuse normal prior $\omega_i \sim \text{normal}(0, 1000)$. The terms ϵ_t and $\gamma_{i,t}$ represent temporally- and spatiotemporally-structured random effects, respectively. The random effects are assumed to be independent with distributions $\epsilon_t \sim \text{normal}(0, \sigma^2_\epsilon)$, $\sigma_\epsilon \sim \text{uniform}(0, 10)$, $\gamma_{i,t} \sim \text{normal}(0, \sigma^2_{\gamma,i})$, and $\sigma_{\gamma,i} \sim \text{uniform}(0, 10)$. The ϵ_t term represents the between-year variation in density that is synchronous to all segments, and the $\gamma_{i,t}$ term represents the variation that is segment-specific (i.e., asynchronous).

Following Grosbois et al. (2009) and Lahoz-Monfort et al. (2011), we used posterior samples of the estimated variances of the two random effect terms to derive a segment-specific intraclass correlation coefficient (ICC):

$$ICC_i = \frac{\hat{\sigma}^2_\epsilon}{\hat{\sigma}^2_\epsilon + \hat{\sigma}^2_{\gamma,i}}\,. \tag{5}$$

The ICC serves as a measure of synchrony of the local population in segment i relative to the temporal variation averaged across all segments. When $\hat{\sigma}^2_\epsilon$ was greater than $\hat{\sigma}^2_{\gamma,i}$, the resulting ICC values >0.5 indicated that the given segment was synchronous with the averaged temporal variation. Conversely, ICC values <0.5 indicated asynchrony. We created semivariograms of YOY and adult ICC values to check for spatial structure in synchrony.

The synchronizing effects of the climate covariates in Eq. (3) can be estimated from the variances of the covariate coefficients ($\boldsymbol{\sigma}^2_\beta$). A coefficient with low variance (that is, similar effects on different populations) was one that has a strong synchronizing effect. A covariate with a high variance (differing effects on different populations) was one with a weak synchronizing effect.

We tested for the the presence of a portfolio of population responses by comparing segment-specific interannual variability in observed abundance to that of all segments following Schindler et al. (2010). We calculated the coefficient of variation in pass 1 YOY abundance for each segment, as well as in the average of pass 1 YOY abundance for all segments. A smaller coefficient of variation across all segments than in individual segments demonstrates a portfolio effect.

We fit a total of twelve models: One random effects and one climate effects model each for YOY and adults at the regional scale fit to all stream segments (hereafter the "regional" models), as well as one random effect model and one climate effect model each for YOY and adults in the northern and southern halves of the study region, hereafter the "sub-regional" models. We implemented our models utilizing Markov Chain Monte Carlo (MCMC) sampling using JAGS with the 'jagsUI' package in R (Kellner, 2021). We link to code in Appendix 4. After a burn-in period of 5,000 samples for the climate effects models and 20,000 for random effects models, three chains were run without thinning until 25,000 and 50,000 iterations were reached, respectively. All chains converged, as visually evaluated using trace plots. To evaluate the performance of our models, we

completed posterior predictive checks for the test statistics of mean and coefficient of variation. These checks test for lack of fit using Bayesian p-values, defined as the probability that simulated data are more extreme than the observed data (Gelman et al., 2004). Using this method, models with a lack of fit produce Bayesian p-values close to 0 or 1. We report posterior means as point estimates and 95% highest posterior density intervals (HPDIs) as estimates of uncertainty. Values were considered significant if their 95% HPDIs did not overlap 0.

3 RESULTS

3.1 Correlogram Analysis

The average scale and magnitude of spatial synchrony in both YOY and adult brook trout was relatively low compared with those of a suite of climate variables (Fig. 2). The 95% CI of initial pairwise correlation did not overlap between trout density and abiotic variables. Correlation lengths measured using the 2.5^{th} percentile of the 95% confidence envelope of the spline correlogram were 84 km in YOY and 70 km in adult brook trout. Point estimates for the scale of synchrony were roughly 150 km for both life stages. Summer air and water temperature and winter streamflow and precipitation were synchronous to scales of 400 km or more. Average pairwise correlations in YOY and adult brook trout were 0.07 and 0.05, respectively, and those of the climate variables ranged from 0.51 to 0.64. Initial pairwise correlation was considerably higher in the northern sub-region for adults (mean = 0.29; 95% CI = 0.14 to 0.47 vs. mean = 0.07; 95% CI = -0.08 to 0.2 for the southern sub-region). However, neither the scale nor average magnitude of synchrony differed greatly between sub-regions (Fig. 3).

3.2 Hierarchical Model

Lacking random effects, predictive ability of the climate effect models was modest. Bayesian p-values for mean and coefficient of variation of pass 1 abundance were 0.2 and 0.92 (YOY) and 0 and 0.99 (adult). Predictive ability of the random effects models was improved considerably because these models accounted for temporal and spatiotemporal variability. Bayesian p-values for mean and coefficient of variation of pass 1 abundance were 0.14 and 0.14 (YOY) and 0.37 and 0.74 (adult). Electrofishing capture probability per pass (p) was higher for adults than YOY. Estimates of capture probability varied by data source, with the mean probability ranging from 0.55 (95%

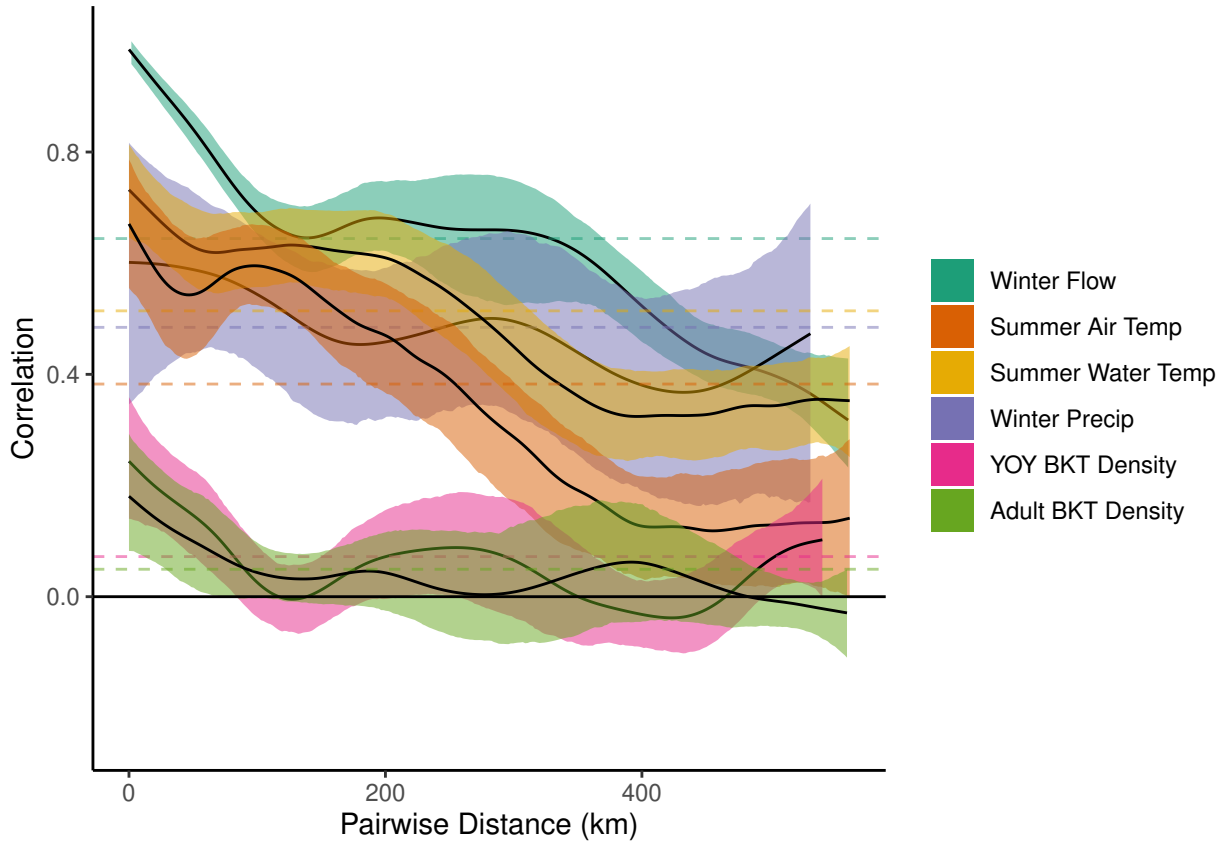

Figure 2: Spline correlogram of pairwise correlation in brook trout (*Salvelinus fontinalis*) density and selected climate variables for the southeast USA. Climate variables: mean estimated monthly winter flow, mean daily observed summer air temperature, mean daily observed summer water temperature, and total observed monthly winter precipitation. Brook trout density is log transformed. Shading indicates 95% confidence envelopes. Dashed lines represent average pairwise correlations. Climate data sources: USGS NHDPlus v2.1, USDA Forest Service, NOAA.

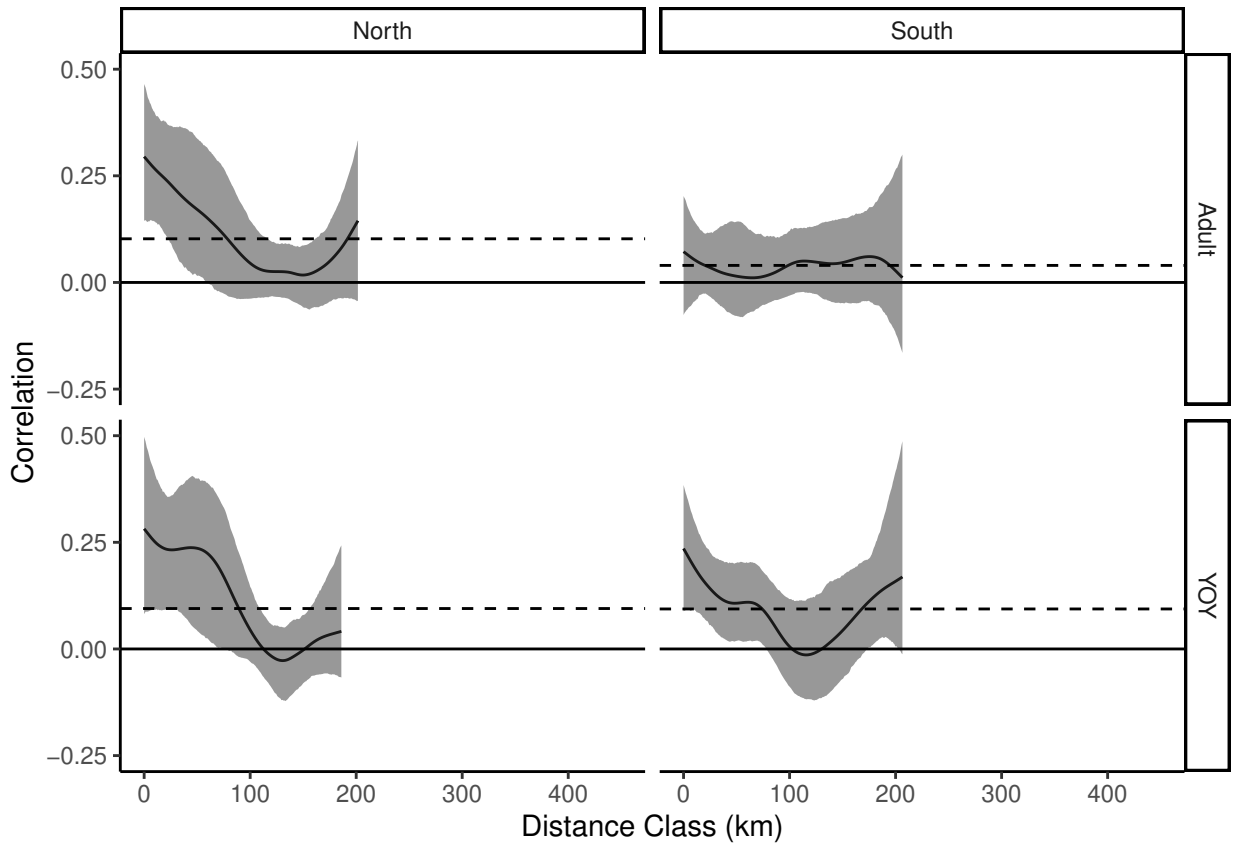

Figure 3: Spline correlogram of log brook trout (*Salvelinus fontinalis*) density by life stage and sub-region. Shaded regions represent 95% confidence envelope. Dashed lines represent average pairwise correlations.

HPDI = 0.52 to 0.58) to 0.85 (95% HPDI = 0.84 to 0.87) for YOY and from 0.69 (95% HPDI = 0.69 to 0.7) to 0.9 (95% HPDI = 0.89 to 0.91) for adults (Fig. S4).

3.2.1 Overall Climate Effects Across Stream Segments

Climate effects on brook trout abundance varied by sub-region and life stage, as represented by posterior distributions of the mean parameters for $\boldsymbol{\mu}_\beta$ (Fig. 4). In all cases, YOY were more affected by climate than were adults, thus unless noted otherwise we focus here on YOY responses. At the regional scale (symbolized in green in Fig. 4), all three environmental covariates had negative effects on YOY abundance, while only summer air temperature had an effect on adult abundance. Winter high flow had the strongest negative effect on YOY abundance (mean = -0.27; 95% HPDI = -0.35 to -0.18), followed by spring high flow (mean = -0.11; 95% HPDI = -0.22 to 0) and high temperatures in the previous summer (mean = -0.09; 95% HPDI = -0.19 to 0).

Covariate effects at the sub-regional scale varied. As hypothesized, air temperature had a stronger effect on YOY in the south than in the north (mean = -0.26; 95% HPDI = -0.39 to -0.13 vs. mean = 0; 95% HPDI = -0.13 to 0.13). Within the northern sub-region (symbolized in orange in Fig. 4), YOY abundance was exclusively driven by flow (winter flow mean = -0.28 and 95% HPDI = -0.4 to -0.18 and spring flow mean = -0.21 and 95% HPDI = -0.34 to -0.07), with no effect of summer air temperature (mean = 0; 95% HPDI = -0.13 to 0.13). Within the southern sub-region (symbolized in purple in Fig. 4), summer air temperature and winter flow had the strongest negative effect on YOY abundance (mean = -0.26; 95% HPDI = -0.39 to -0.13 and mean = -0.23; 95% HPDI = -0.36 to -0.09). The effect of spring flows on YOY density in the south trended positive (mean = 0.08; 95% HPDI = -0.11 to 0.26). A slight overall negative effect of summer air temperature on adult abundance (mean = -0.04; 95% HPDI = -0.1 to 0.01) was driven by the response of northern populations (mean = -0.05; 95% HPDI = -0.11 to 0.01).

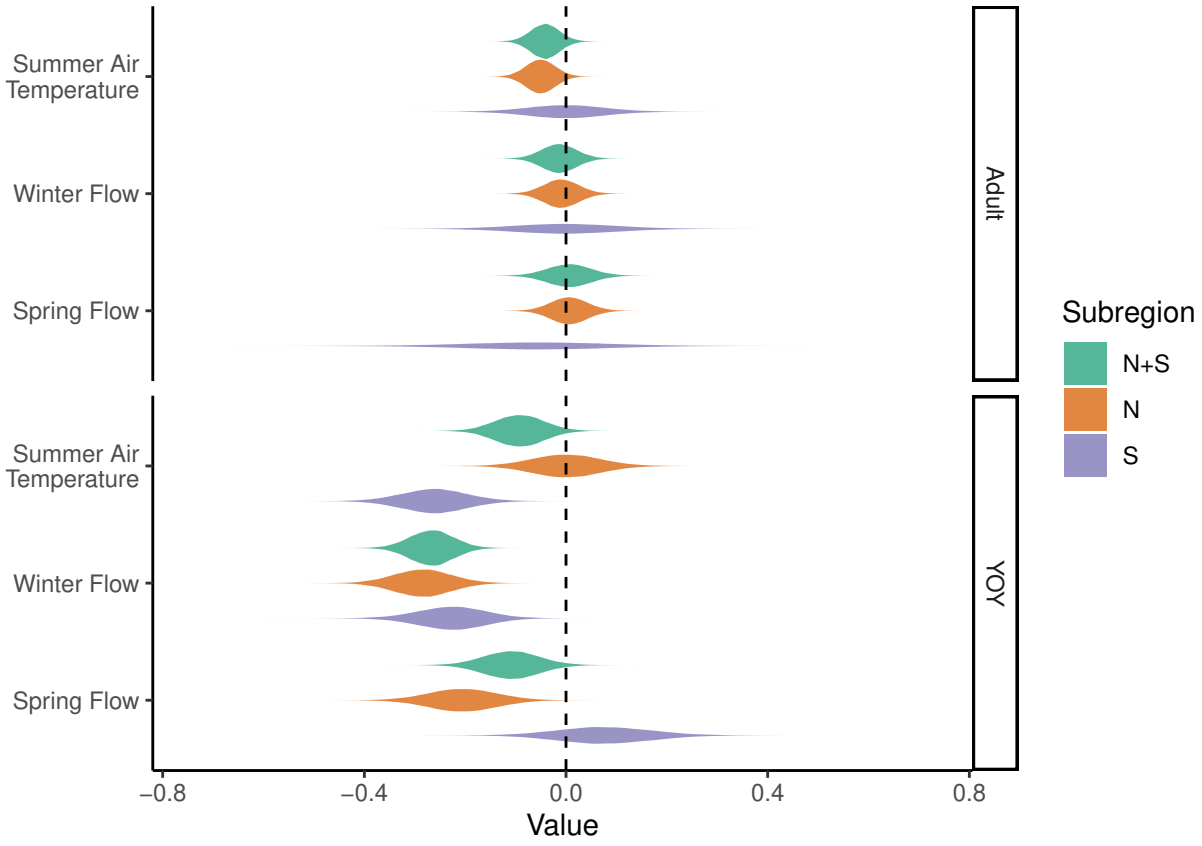

Figure 4: Full posterior distributions for climate effects on brook trout (*Salvelinus fontinalis*) log density by life stage and sub-region. Climate variables: average 0.9Q summer air temperature (year t-1), max 0.9Q winter stream flow (year t), max 0.9Q spring stream flow (year t). Data sources: USGS NHDPlus v2.1, NOAA.

Uncertainty in climate effects on adults in southern populations was much greater than that of northern populations (Fig. 4). Overall, winter and spring stream flows were the primary driver of YOY abundance over time in the northern sub-region, whereas summer air temperature and winter stream flow were the most important drivers of YOY abundance in the southern sub-region.

3.2.2 Spatial Heterogeneity in Climate Effects

Climate effects varied considerably among stream segments (Fig. 5). With this cross-scale interaction, some experienced positive effects, while others experienced negative effects. The variance in local effects ($\boldsymbol{\sigma}^2_{\beta}$) for winter stream flow on YOY abundance (mean = 0.3; 95% HPDI = 0.2 to 0.4) was smaller than that of spring stream flow (mean = 0.5; 95% HPDI = 0.3 to 0.6) or summer temperature (mean = 0.4; 95% HPDI = 0.3 to 0.5; Fig. 5). Summer temperature had the smallest variance in local effects on adult abundance (mean = 0.1 (95% HPDI = 0.1 to 0.2), compared to 0.2 (95% HPDI = 0.1 to 0.2) for winter stream flow and 0.3 (95% HPDI = 0.2 to 0.4) for spring stream flow). Mean variance in climate effects on YOY was higher than that of adults (mean = 0.4 vs. 0.2). Correlation analysis demonstrated that there was little influence of local habitat on model $\boldsymbol{\beta_i}$ (Table S2). There was no notable spatial structure in covariate effects on YOY brook trout abundance (model $\boldsymbol{\beta_i}$, Fig. S5).

3.2.3 Synchrony

Estimates of segment-specific ICC values varied from 0.04 (95% HPDI = 0 to 0.16) to 0.67 (95% HPDI = 0.13 to 1) for YOY brook trout and from 0 (95% HPDI = 0 to 0.01) to 0.67 (95% HPDI = 0.19 to 1) for adult brook trout. YOY brook trout showed higher average ICC than adult brook trout (0.31 vs. 0.14). On average, northern brook trout populations were more synchronous than southern populations (average YOY ICC: 0.31 vs. 0.2). There was little correlation between ICC

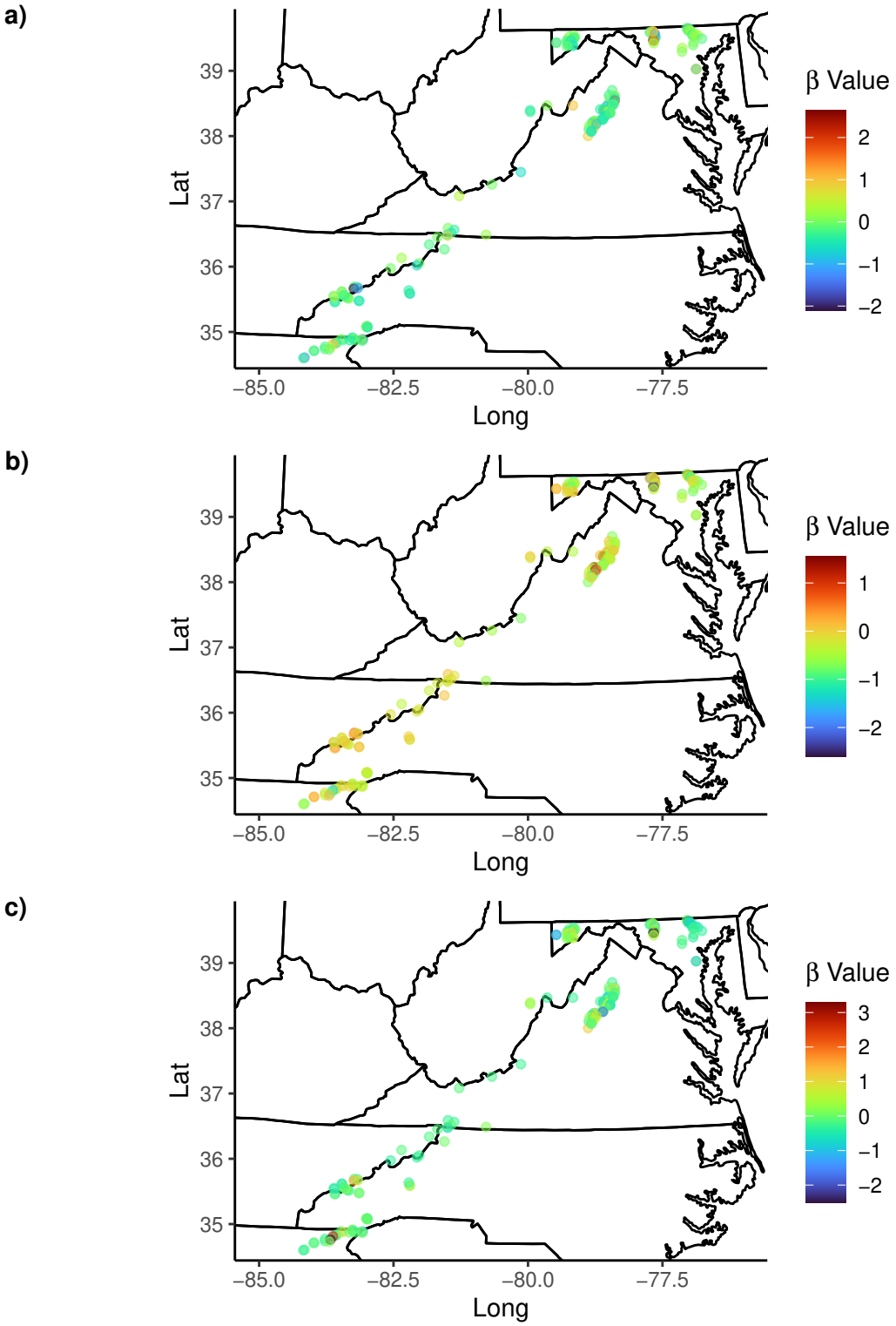

Figure 5: Local climate effects on brook trout (*Salvelinus fontinalis*) young-of-the-year abundance (model β_i). a) average 0.9Q summer air temperature (year t-1), b) max 0.9Q winter stream flow (year t), and c) max 0.9Q spring stream flow (year t). Data sources: USGS NHDPlus v2.1, NOAA.

and local habitat variables (Table S3). Several of the most synchronous populations (highest YOY ICC) were in northeast of the study region (Fig. 6, but see Fig. S7 for adult ICCs). There was considerable geographic heterogeneity in spatial synchrony (Fig. 6), and segment-specific synchrony showed moderate spatial structure (Fig. S6), showing that populations nearer to each other are more similar in temporal abundance patterns than populations farther from each other. Variability in average abundance across all stream segments was lower than in individual segments (Fig. S9), indicating the presence of a portfolio effect among the sampled populations. The coefficient of variation for interannual observed pass 1 abundance for YOY brook trout averaged across segments was 0.62, compared to a mean of 1.13 for individual segments.

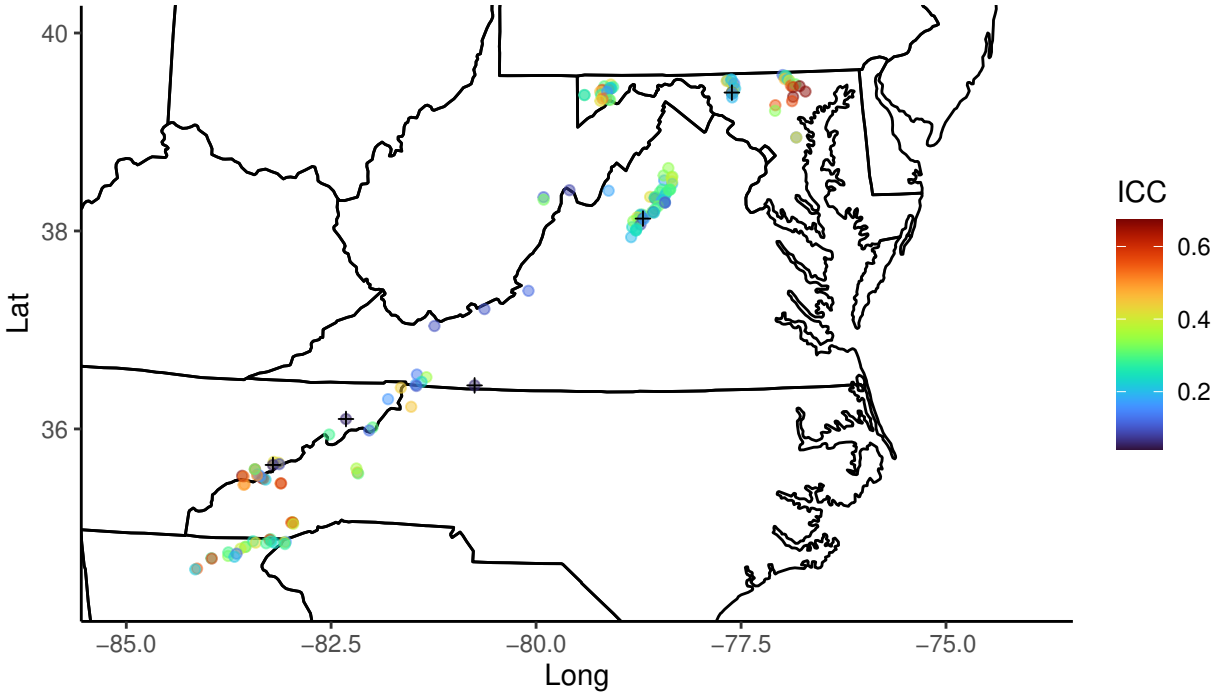

Figure 6: Intraclass correlation coefficient (ICC) values for populations of young-of-the-year brook trout (*Salvelinus fontinalis*) in the southeastern USA. High ICC values indicate synchrony relative to the temporal variation averaged across segments, while low ICC values indicate asynchrony. The five stream segments with lowest ICC (least synchronous) are indicated by "+".

4 DISCUSSION

Synthesizing data from nine public and private data sources at 170 sites over 34 years, this study provides one of the most thorough attempts to understand spatiotemporal variation of stream fish populations across a large geographic region (~1,000 km). We found that a) spatial synchrony in populations of this threatened stream salmonid was only moderate, b) multiple cross-scale interactions with climate influences created heterogeneous population responses across the study area, and c) brook trout life stages differed in both demographic (abundance and density) and emergent (synchrony and asynchrony) reactions to climate influence. Our results build on those of previous studies (e.g., Copeland & Meyer, 2011; Kanno et al., 2015; Kanno et al., 2016; Zorn & Nuhfer, 2007) by quantifying autocorrelation using multiple established methods and expanding the area of study to encompass the entire range edge of this valuable species. We continue to establish the importance of subannual (season-specific, e.g., Letcher et al., 2015) effects in ecological research as well as explore the existence of multi-scale and nested interactions. Lastly, our findings compliment recent genetic research that emphasizes fine-scale population structure in stream salmonids (Kazyak et al., 2022). Our work highlights an opportunity and the need for embracing spatially heterogeneous population responses in range-wide planning for brook trout and other species of conservation concern.

Spatial synchrony in southeast US brook trout populations was low, especially when compared to highly synchronous climate variables such as temperature, precipitation, and flow. Average ICC values for YOY and adult fish were similar to those reported for other freshwater fish species (e.g., Michaletz & Siepker, 2013; Midway & Peoples, 2019) and considerably lower than estimates made for terrestrial species (e.g., Canu et al., 2015; Grosbois et al., 2009; Lahoz-Monfort et al., 2011). This is logical, as aquatic systems more closely meet assumptions of closure than do terres-

trial ones. Climate is often considered to exert strong effects on temporal variation in animal and plant population size (Koenig, 2002; Saether et al., 2004; Stenseth et al., 2002). Consequently, we hypothesized that patterns of spatial synchrony in the spline correlogram would be similar between climate variables and trout populations, if climate exerted a strong effect on population trajectories across space via the Moran Effect. Initial and average correlation among observed precipitation and temperature was over twice as strong as correlation among trout populations, and the spatial scale of synchrony in observed climate was also more than twice that of brook trout. Patterns of synchrony were moderately similar between abiotic and biotic factors, suggesting that these climate variables are exerting a moderate synchronizing effect on populations of brook trout. The spline correlogram for juvenile density exhibited the most similar shape to that of winter flow, with a defined dip at around 150 km. The variance in local effects of winter stream flow on juvenile abundance was also the smallest of the three climate variables in the climate effects model. This implies that winter stream flow is the strongest driver of what little synchrony is present in these populations. Winter stream flow has been suggested as a driver synchrony in other stream salmonids (Cattanéo et al., 2003). The strength of spatial autocorrelation may have differed between the biotic and abiotic responses because trout populations responded to climate heterogeneously over space.

Synchrony was heterogeneous in space, as well as in population structure. Synchrony varied across the landscape, revealing both regional and local diversity in synchrony (Figs. 6). On average, northern populations were considerably more synchronous than southern populations, likely a result of sub-regional differences in population responses to climate. This could be due to genetic differences between these populations (Kazyak et al., 2022). As the more threatened sub-regional population (Flebbe et al., 2006; Kazyak et al., 2022), southern Appalachian brook trout may benefit from their relative asynchrony. The most synchronous populations were located

in eastern Maryland and in Great Smoky Mountain National Park (Fig. 5), however there were no characteristics of local habitat that particularly distinguished these stream segments. Life stage differences in synchrony were also apparent. YOY fish populations were more than twice as synchronous than adults, supporting prior indications that YOY brook trout experience higher synchrony than adults (Kanno et al., 2016). This pattern of stronger synchrony in juvenile life stages is well-reflected in the literature, occurring in fish taxa from other salmonids (Cattanéo et al., 2003) to warm water and shoaling fish (Grenouillet et al., 2001; Reyjol et al., 2008).

It is important to recognize that inferences in population synchrony and heterogeneous responses depend inherently on geographic extent of investigations (Levin, 1992; Wiens, 1989), demonstrated similarly by our parallel analyses of regional versus sub-regional data. In brook trout, previous studies have reported stronger magnitude of spatial population synchrony than the current study, but they were much more limited in geographic extent (Kanno et al., 2016; Zorn & Nuhfer, 2007). Estimates of the spatial scale of synchrony in freshwater populations vary widely (Copeland & Meyer, 2011; Myers et al., 1997), however our estimates were in line with previous studies of brook trout (Kanno et al., 2016; Zorn & Nuhfer, 2007), as well as with other freshwater species (Tedesco et al., 2004). Our macro-scale patterns emerged through analyses of multiple spatially and temporally replicated data sets (170 stream segments over 34 years) dispersed across over 1,000 km, and they provide a unique synthesis of climate vulnerability of this sensitive coldwater fish.

Our analysis revealed that climatic patterns in summer temperature and winter and spring flow explained temporal variation in early-life-stage abundance, supporting the notion that cold-water stream fish in their range edges are particularly sensitive to extremes of temperature and flow (Santiago et al., 2017). Climate change is expected to bring warmer air temperatures and increased precipitation to the southeast USA (Alipour et al., 2020; Ingram et al., 2013; Pörtner et

al., 2022). Based on these projections, we expect decreased recruitment and increased mortality of YOY brook trout in the future. Climate variables affected abundance of young-of-the-year trout more than adult trout over time. Life-stage-specific responses to stream flows are well documented in stream salmonids (Cattanéo et al., 2003; Kanno et al., 2017; Kovach et al., 2016). Early life stages of trout suffer high mortality when elevated flows mobilize stream bed substrates, as corroborated by diminished young-of-the-year abundance in summer following wet winter and spring in this fall-spawning species. These findings support our hypothesis that stream flow would have a stronger effect on the juvenile life stage than the adult stage. We also observed that young-of-the-year abundance in southern populations decreased following a hot summer in the previous year. This pattern is less frequently documented in stream salmonids than are flow effects (Kovach et al., 2016). A potential mechanism is high adult mortality due to elevated summer temperature, which would lead to low spawner abundance in fall. Our data show that adult abundance was moderately sensitive to temperature in the previous summer, however this was in the northern populations, rather than the south, where juveniles experienced temperature effects. While low spawner abundance can result in low recruitment, higher spawner abundance does not always result in higher recruitment in brook trout (Grossman et al., 2010; Kanno et al., 2016; Sweka & Wagner, 2022). We observed a positive trend between spawner abundance and recruitment (Fig. S8). Alternatively, this species delays or skips spawning in fall following hot summer (Warren et al., 2012), and this sub-lethal effect could lead to lower YOY abundance in the following year. Regardless of mechanisms, heterogeneous responses to climate variables between life stages may provide a demographic portfolio effect (Dybala et al., 2013; Schindler et al., 2010; Schindler et al., 2015), which can buffer brook trout populations from thermal and flow alterations to some extent.

Climate effects on temporal animal abundance differed geographically at both broad and fine spatial scales, demonstrating multiple cross-scale interactions. As hypothesized, elevated tem-

perature in the previous summer explained temporal variation in young-of-the-year brook trout abundance in the southern sub-region more strongly than in the northern sub-region. Populations of this coldwater fish inhabiting the southern extent of their range were indeed more sensitive to elevated temperatures. While spring flows had a negative effect on juvenile abundance in the south, they trended positive for juvenile abundance in the north. With earlier hatch dates, trout in southern populations may be more able to withstand late spring flows than those in northern populations.

Within these broad-scale interactions, we also observed interactions at fine scales. While regional and sub-regional climate effects were mostly negative, individual population responses varied. Several populations had strong negative responses, while others experienced positive responses to climate - particularly spring flow. Our exploratory analysis between segment-specific climate effects ($\boldsymbol{\beta}$) and spatial covariates (e.g., elevation, watershed area, channel slope) did not identify their linkages. This lack of correlation suggests that other factors may be responsible for the observed complex cross-scale interactions (Soranno et al., 2014). One possibility is population diversity: Southern Appalachian brook trout show considerable diversity even within and among drainages (Kazyak et al., 2022). Genetic lineages may respond differently to environmental conditions - an important consideration in the determination of evolutionarily significant units (Kazyak et al., 2022; Nielsen, 1995; Waples, 1991). Another possibility is an unobserved local habitat factor. Groundwater, for one, is an aspect of local habitat that can buffer the negative effects of temperature and flow (Brunke et al., 2003; Cartwright & Johnson, 2018). It can also provide superior spawning and rearing habitat for fish (Blanchfield & Ridgway, 1997; Curry & Noakes, 1995). Groundwater influence, however, remains difficult to measure and predict over broad spatial scales (Kalbus et al., 2006). Likewise, stream shading and riparian vegetation are highly local habitat factors that are difficult to measure at broad scales but can buffer temperature and flooding. In fact, increasing

evidence suggests that it is this highly local habitat heterogeneity combined with diverse population responses that buffers synchrony and increases resilience via a portfolio effect (Hilborn et al., 2003; Schindler et al., 2010; Schindler et al., 2015). This heterogeneity may also create climate refugia, critical to the long-term persistence of native species (Larios-López et al., 2020; Morelli et al., 2020). Climate refugia are of growing importance in ecological studies. They are typically identified by local abiotic characteristics (Ashcroft, 2010; Cartwright & Johnson, 2018). However, a commonly identified weakness with traditional approaches to identifying refugia is that verification is seldom carried out (Barrows et al., 2020). By identifying asynchronous populations, we can identify potential refugia using empirical biotic evidence, thus verifying their ecological function. Our methods allow us to identify locations and populations that are potentially resilient to climate stressors.

We fit two separate removal N-mixture models (i.e., climate effects models and random effects models). While this approach helps achieve model convergence (and our simulations suggest that parameters of models combining them should be identifiable), it has consequences for the range of possible inferences to be made. With no climate covariates in the random effects models, the two random effects absorb all temporal and spatiotemporal variance in density, and we cannot conclusively attribute spatial synchrony to specific climate drivers. Conversely, models lacking random effects overestimate the precision (i.e., underestimate 95% credible intervals) of regression coefficients such as climate covariate effects in our study, but their point estimates (i.e., posterior means) are much less affected (Schaub & Kéry, 2012). Therefore, our analysis should provide reliable inferences on the relative importance of temperature and flow effects and their spatial variation on trout abundance.

Spatially heterogeneous and asynchronous population responses to climate have implications for the conservation of this and other threatened species at their range edges. Previous stud-

ies assumed homogeneous and synchronous population responses to climate change in salmonids (Meisner, 1990; Rahel et al., 1996), and up to 97% habitat loss was projected for brook trout populations in the southern Appalachian Mountain streams (Flebbe et al., 2006), which corresponds to the southern sub-region of our current study. Although climate change is undeniably a major threat to sensitive coldwater fish, our results demonstrate the importance of considering spatial heterogeneity and recognizing that some populations are more likely to persist than others in a changing climate. A key challenge lies in identifying a set of priority conservation populations in a landscape in an increasingly uncertain and non-stationary environment (Heller & Zavaleta, 2009). Our results inform this challenge. In this study and others, a portfolio effect diminished temporal variation in region-scale abundance (Hilborn et al., 2003; Schindler et al., 2010; Schindler et al., 2015). Similar to the manner in which Essential Fish Habitat is identified and conserved in some marine jurisdictions (Rosenberg et al., 2000), priority conservation populations may be identified from gradients of population synchrony and heterogeneity to climate variation, so that a portfolio of populations with a range of climate responses may be targeted for protection and restoration to buffer against climate change impacts. This approach is applicable to other wide-ranging species with spatially and temporally replicated data sets.

REFERENCES

Alipour, A., Ahmadalipour, A., & Moradkhani, H. (2020). Assessing flash flood hazard and damages in the southeast United States. *Journal of Flood Risk Management*, *13*(2), e12605. https://doi.org/10.1111/jfr3.12605

American Sportfishing Association, & Sport Fish Restoration. (2021). *Sportfishing in America: A Reliable Economic Force*.

Ashcroft, M. B. (2010). Identifying refugia from climate change. *Journal of Biogeography*, *37*(8), 1407–1413. https://doi.org/10.1111/j.1365-2699.2010.02300.x

Barrows, C. W., Ramirez, A. R., Sweet, L. C., Morelli, T. L., Millar, C. I., Frakes, N., Rodgers, J., & Mahalovich, M. F. (2020). Validating climate-change refugia: Empirical bottom-up approaches to support management actions. *Frontiers in Ecology and the Environment*, *18*(5), 298–306. https://doi.org/10.1002/fee.2205

Benda, L., Poff, N. L., Miller, D., Dunne, T., Reeves, G., Pess, G., & Pollock, M. (2004). The network dynamics hypothesis: How channel networks structure riverine habitats. *BioScience*, *54*(5), 413–427. https://doi.org/10.1641/0006-3568(2004)054%5B0413:TNDHHC%5D2.0.CO;2

Berliner, L. M. (1996). Hierarchical Bayesian Time Series Models. In K. M. Hanson & R. N. Silver (Eds.), *Maximum Entropy and Bayesian Methods* (pp. 15–22). Springer Netherlands. https://doi.org/10.1007/978-94-011-5430-7_3

Bjornstad, O. N. (2022). *Ncf: Spatial Covariance Functions*.

Bjørnstad, O. N., & Falck, W. (2001). Nonparametric spatial covariance functions: Estimation and testing. *Environmental and Ecological Statistics*, *8*(1), 53–70. https://doi.org/10.1023/A:1009601932481

Blanchfield, P. J., & Ridgway, M. S. (1997). Reproductive timing and use of redd sites by lake-spawning brook trout (Salvelinus fontinalis). *Canadian Journal of Fisheries and Aquatic Sciences*, *54*(4), 747–756. https://doi.org/10.1139/f96-344

Boddy, N. C., Booker, D. J., & McIntosh, A. R. (2019). Confluence configuration of river networks controls spatial patterns in fish communities. *Landscape Ecology*, *34*(1), 187–201. https://doi.org/10.1007/s10980-018-0763-4

Brunke, M., Hoehn, E., & Gonser, T. (2003). Patchiness of river–groundwater interactions within two floodplain landscapes and diversity of aquatic invertebrate communities. *Ecosystems*, *6*(8), 707–722. https://doi.org/10.1007/PL00021501

Canu, A., Scandura, M., Merli, E., Chirichella, R., Bottero, E., Chianucci, F., Cutini, A., & Apollonio, M. (2015). Reproductive phenology and conception synchrony in a natural wild boar population. *Hystrix*, *26*(2), 77–84. https://doi.org/10.4404/hystrix-26.2-11324

Cartwright, J., & Johnson, H. M. (2018). Springs as hydrologic refugia in a changing climate? A remote-sensing approach. *Ecosphere*, *9*(3), e02155. https://doi.org/10.1002/ecs2.2155

Cattanéo, F., Hugueny, B., & Lamouroux, N. (2003). Synchrony in brown trout, Salmo trutta, population dynamics: A 'Moran effect' on early-life stages. *Oikos*, *100*(1), 43–54. https://doi.org/10.1034/j.1600-0706.2003.11912.x

Cattanéo, F., Lamouroux, N., Breil, P., & Capra, H. (2002). The influence of hydrological and biotic processes on brown trout (Salmo trutta) population dynamics. *Canadian Journal of Fisheries and Aquatic Sciences*, *59*(1), 12–22. https://doi.org/10.1139/f01-186

Childress, E. S., Nislow, K. H., Whiteley, A. R., O'Donnell, M. J., & Letcher, B. H. (2019). Daily estimates reveal fine-scale temporal and spatial variation in fish survival across a stream network. *Canadian Journal of Fisheries and Aquatic Sciences*, *76*(8), 1446–1458. https://doi.org/10.1139/cjfas-2018-0191

Cline, T. J., Muhlfeld, C. C., Kovach, R., Al-Chokhachy, R., Schmetterling, D., Whited, D., &

Lynch, A. J. (2022). Socioeconomic resilience to climatic extremes in a freshwater fishery. *Science Advances*, *8*(36), eabn1396. https://doi.org/10.1126/sciadv.abn1396

Copeland, T., & Meyer, K. A. (2011). Interspecies synchrony in salmonid densities associated with large-scale bioclimatic conditions in central idaho. *Transactions of the American Fisheries Society*, *140*(4), 928–942. https://doi.org/10.1080/00028487.2011.599261

Curry, R. A., & Noakes, D. L. G. (1995). Groundwater and the selection of spawning sites by brook trout (Salvelinus fontinalis). *Canadian Journal of Fisheries and Aquatic Sciences*, *52*(8), 1733–1740. https://doi.org/10.1139/f95-765

Donald, D. B., & Alger, D. J. (1989). Evaluation of exploitation as a means of improving growth in a stunted population of Brook Trout. *North American Journal of Fisheries Management*, *9*(2), 177–183. https://doi.org/10.1577/1548-8675(1989)009%3C0177:EOEAAM%3E2.3.CO;2

Dybala, K. E., Eadie, J. M., Gardali, T., Seavy, N. E., & Herzog, M. P. (2013). Projecting demographic responses to climate change: Adult and juvenile survival respond differently to direct and indirect effects of weather in a passerine population. *Global Change Biology*, *19*(9), 2688–2697. https://doi.org/10.1111/gcb.12228

Eastern Brook Trout Joint Venture. (2006). *Eastern brook trout: Status and threats*.

Eaton, J. G., McCormick, J. H., Goodno, B. E., O'Brien, D. G., Stefany, H. G., Hondzo, M., & Scheller, R. M. (1995). A field information-based system for estimating fish temperature tolerances. *Fisheries*, *20*(4), 10–18. https://doi.org/10.1577/1548-8446(1995)020%3C0010:afisfe%3E2.0.co;2

Flebbe, P. A., Roghair, L. D., & Bruggink, J. L. (2006). Spatial modeling to project southern appalachian trout distribution in a warmer climate. *Transactions of the American Fisheries Society*, *135*(5), 1371–1382. https://doi.org/10.1577/t05-217.1

Fletcher, R., Fortin, M.-J., Fletcher, R., & Fortin, M.-J. (2018). Population Dynamics in Space. In *Spatial Ecology and Conservation Modeling* (pp. 369–417). Springer International Publishing. https://doi.org/10.1007/978-3-030-01989-1_10

Fridley, J. D. (2009). Downscaling climate over complex terrain: High finescale (<1000 m) spatial variation of near-ground temperatures in a montane forested landscape (great smoky mountains). *Journal of Applied Meteorology and Climatology*, *48*(5), 1033–1049. https://doi.org/10.1175/2008JAMC2084.1

Frissell, C. A., Liss, W. J., Warren, C. E., & Hurley, M. D. (1986). A hierarchical framework for stream habitat classification: Viewing streams in a watershed context. *Environmental Management*, *10*(2), 199–214. https://doi.org/10.1007/BF01867358

Gelman, A., Carlin, J. B., Stern, H. S., & Rubin, D. B. (2004). *Bayesian Data Analysis*. Chapman and Hall/CRC.

Goode, J. R., Buffington, J. M., Tonina, D., Isaak, D. J., Thurow, R. F., Wenger, S., Nagel, D., Luce, C., Tetzlaff, D., & Soulsby, C. (2013). Potential effects of climate change on streambed scour and risks to salmonid survival in snow-dominated mountain basins. *Hydrological Processes*, *27*(5), 750–765. https://doi.org/10.1002/hyp.9728

Grenouillet, G., Hugueny, B., Carrel, G. A., Olivier, J. M., & Pont, D. (2001). Large-scale synchrony and inter-annual variability in roach recruitment in the Rhône River: The relative role of climatic factors and density-dependent processes. *Freshwater Biology*, *46*(1), 11–26. https://doi.org/10.1046/j.1365-2427.2001.00637.x

Grosbois, V., Harris, M. P., Anker-Nilssen, T., Mccleery, R. H., Shaw, D. N., Morgan, B. J. T., & Gimenez, O. (2009). Modeling survival at multi-population scales using mark-recapture data. *Ecology*, *90*(10), 2922–2932. https://doi.org/10.1890/08-1657.1

Grossman, G. D., Ratajczak, R. E., Wagner, C. M., & Petty, J. T. (2010). Dynamics and regulation of the southern brook trout (Salvelinusfontinalis) population in an Appalachian stream.

Freshwater Biology, *55*(7), 1494–1508. https://doi.org/10.1111/j.1365-2427.2009.02361.x

Hampe, A., & Petit, R. J. (2005). Conserving biodiversity under climate change: The rear edge matters. *Ecology Letters*, *8*(5), 461–467. https://doi.org/10.1111/j.1461-0248.2005.00739.x

Hansen, B. B., Grøtan, V., Herfindal, I., & Lee, A. M. (2020). The Moran Effect revisited: Spatial population synchrony under global warming. *Ecography*, *43*(11), 1591–1602. https://doi.org/10.1111/ecog.04962

Hazzard, A. S. (1932). Some phases of the life history of the Eastern Brook Trout, Salvelinus fontinalis mitchell. *Transactions of the American Fisheries Society*, *62*(1), 344–350. https://doi.org/10.1577/1548-8659(1932)62%5B344:SPOTLH%5D2.0.CO;2

Heino, M., Kaitala, V., Ranta, E., & Lindstrom, J. (1997). Synchronous dynamics and rates of extinction in spatially structured populations. *Proceedings of the Royal Society B: Biological Sciences*, *264*(1381), 481–486. https://doi.org/10.1098/rspb.1997.0069

Heller, N. E., & Zavaleta, E. S. (2009). Biodiversity management in the face of climate change: A review of 22 years of recommendations. *Biological Conservation*, *142*(1), 14–32. https://doi.org/10.1016/j.biocon.2008.10.006

Herfindal, Lee AM, Marquez JF, Le Moullec M, Peeters B, Hansen BB, Henden JA, & Sæther BE. (2022). Environmental effects on spatial population dynamics and synchrony: Lessons from northern ecosystems. *Climate Research*, *86*, 113–123.

Hilborn, R., Quinn, T. P., Schindler, D. E., & Rogers, D. E. (2003). Biocomplexity and fisheries sustainability. *Proceedings of the National Academy of Sciences*, *100*(11), 6564–6568. https://doi.org/10.1073/pnas.1037274100

Hudy, M., Coombs, J. A., Nislow, K. H., & Letcher, B. H. (2010). Dispersal and within-stream spatial population structure of brook trout revealed by pedigree reconstruction analysis. *Transactions of the American Fisheries Society*, *139*(5), 1276–1287. https://doi.org/10.1577/T10-027.1

Hudy, M., Thieling, T. M., Gillespie, N., & Smith, E. P. (2008). Distribution, status, and land use characteristics of subwatersheds within the native range of brook trout in the eastern united states. *North American Journal of Fisheries Management*, *28*(4), 1069–1085. https://doi.org/10.1577/m07-017.1

Hufkens, K., Basler, D., Milliman, T., Melaas, E. K., & Richardson, A. D. (2018). An integrated phenology modelling framework in R. *Methods in Ecology and Evolution*, *9*(5), 1276–1285. https://doi.org/10.1111/2041-210X.12970

Hughes, R. M., Kaufmann, P. R., Herlihy, A. T., Intelmann, S. S., Corbett, S. C., Arbogast, M. C., & Hjort, R. C. (2002). Electrofishing distance needed to estimate fish species richness in raftable Oregon rivers. *North American Journal of Fisheries Management*, *22*(4), 1229–1240. https://doi.org/10.1577/1548-8675(2002)022%3C1229:EDNTEF%3E2.0.CO;2

Ingram, K. T., Dow, K., Carter, L., Anderson, J., & Sommer, E. K. (2013). *Climate of the Southeast United States: Variability, change, impacts, and vulnerability*. Springer.

Isaak, D. J., Wenger, S. J., Peterson, E. E., Ver Hoef, J. M., Nagel, D. E., Luce, C. H., Hostetler, S. W., Dunham, J. B., Roper, B. B., Wollrab, S. P., Chandler, G. L., Horan, D. L., & Parkes-Payne, S. (2017). The NorWeST summer stream temperature model and scenarios for the western U.S.: A crowd-sourced database and new geospatial tools foster a user community and predict broad climate warming of rivers and streams. *Water Resources Research*, *53*(11), 9181–9205. https://doi.org/10.1002/2017WR020969

Kalbus, E., Reinstorf, F., & Schirmer, M. (2006). Measuring methods for groundwater-surface water interactions: A review. *Hydrology and Earth System Sciences*, *10*(6), 873–887. https://doi.org/10.5194/hess-10-873-2006

Kanno, Y., Kulp, M. A., Moore, S. E., & Grossman, G. D. (2017). Native brook trout and invasive rainbow trout respond differently to seasonal weather variation: Spawning timing matters.

Freshwater Biology, *62*(5), 868–879. https://doi.org/10.1111/fwb.12906

Kanno, Y., Letcher, B. H., Hitt, N. P., Boughton, D. A., Wofford, J. E. B., & Zipkin, E. F. (2015). Seasonal weather patterns drive population vital rates and persistence in a stream fish. *Global Change Biology*, *21*(5), 1856–1870. https://doi.org/10.1111/gcb.12837

Kanno, Y., Pregler, K. C., Hitt, N. P., Letcher, B. H., Hocking, D. J., & Wofford, J. E. B. (2016). Seasonal temperature and precipitation regulate brook trout young-of-the-year abundance and population dynamics. *Freshwater Biology*, *61*(1), 88–99. https://doi.org/10.1111/fwb.12682

Kazyak, D. C., Lubinski, B. A., Kulp, M. A., Pregler, K. C., Whiteley, A. R., Hallerman, E., Coombs, J. A., Kanno, Y., Rash, J. M., Morgan II, R. P., Habera, J., Henegar, J., Weathers, T. C., Sell, M. T., Rabern, A., Rankin, D., & King, T. L. (2022). Population genetics of Brook Trout in the southern Appalachian Mountains. *Transactions of the American Fisheries Society*, *151*(2), 127–149. https://doi.org/10.1002/tafs.10337

Kellner, K. (2021). *jagsUI: A Wrapper Around 'rjags' to Streamline 'JAGS' Analyses*.

Kimmel, W. G., & Argent, D. G. (2006). Efficacy of two-pass electrofishing employing multiple units to assess stream fish species richness. *Fisheries Research*, *82*(1), 14–18. https://doi.org/10.1016/j.fishres.2006.09.001

Koenig, W. D. (1999). Spatial autocorrelation of ecological phenomena. *Trends in Ecology and Evolution*, *14*(1), 22–26. https://doi.org/10.1016/S0169-5347(98)01533-X

Koenig, W. D. (2002). Global patterns of environmental synchrony and the Moran Effect. *Ecography*, *25*(3), 283–288. https://doi.org/10.1034/j.1600-0587.2002.250304.x

Koenig, W. D., & Knops, J. M. H. (1998). Scale of mast-seeding and tree-ring growth. *Nature*, *396*(6708), 225–226. https://doi.org/10.1038/24293

Kovach, R. P., Muhlfeld, C. C., Al-Chokhachy, R., Dunham, J. B., Letcher, B. H., & Kershner, J. L. (2016). Impacts of climatic variation on trout: A global synthesis and path forward. *Reviews in Fish Biology and Fisheries*, *26*(2), 135–151. https://doi.org/10.1007/s11160-015-9414-x

Lahoz-Monfort, J. J., Morgan, B. J. T., Harris, M. P., Wanless, S., & Freeman, S. N. (2011). A capture-recapture model for exploring multi-species synchrony in survival. *Methods in Ecology and Evolution*, *2*(1), 116–124. https://doi.org/10.1111/j.2041-210X.2010.00050.x

Larios-López, J. E., Alonso González, C., Galiana-García, M., & Tierno de Figueroa, J. M. (2020). Driving factors of synchronous dynamics in brown trout populations at the rear edge of their native distribution. *Ecology of Freshwater Fish*, *August 2019*, 1–14. https://doi.org/10.1111/eff.12554

Larson, G. L., & Moore, S. E. (1985). Encroachment of exotic Rainbow Trout into stream populations of native Brook Trout in the southern Appalachian Mountains. *Transactions of the American Fisheries Society*, *114*(2), 195–203. https://doi.org/10.1577/1548-8659(1985)114%3C195:eoerti%3E2.0.co;2

Letcher, B. H., Schueller, P., Bassar, R. D., Nislow, K. H., Coombs, J. A., Sakrejda, K., Morrissey, M., Sigourney, D. B., Whiteley, A. R., O'Donnell, M. J., & Dubreuil, T. L. (2015). Robust estimates of environmental effects on population vital rates: An integrated capture–recapture model of seasonal brook trout growth, survival and movement in a stream network. *Journal of Animal Ecology*, *84*(2), 337–352. https://doi.org/10.1111/1365-2656.12308

Levin, S. A. (1992). The problem of pattern and scale in ecology: The Robert H. MacArthur Award lecture. *Ecology*, *73*(6), 1943–1967. https://doi.org/10.2307/1941447

Li, H., Deng, X., Dolloff, C. A., & Smith, E. P. (2016). Bivariate functional data clustering: Grouping streams based on a varying coefficient model of the stream water and air temperature relationship. *Environmetrics*, *27*(1), 15–26. https://doi.org/10.1002/env.2370

Liebhold, A., Koenig, W. D., & Bjornstad, O. N. (2004). Spatial synchrony in population dynamics. *Annual Review of Ecology, Evolution and Systematics*, *35*(2004), 467–490. https://doi.org/10.

2307/annurev.ecolsys.34.011802.30000018

Lloyd, N. J., Mac Nally, R., & Lake, P. S. (2005). Spatial autocorrelation of assemblages of benthic invertebrates and its relationship to environmental factors in two upland rivers in southeastern Australia. *Diversity and Distributions*, *11*(5), 375–386. https://doi.org/10.1111/j.1366-9516.2005.00166.x

Lobón-Cerviá, J. (2007). Numerical changes in stream-resident brown trout (Salmo trutta): Uncovering the roles of density-dependent and density-independent factors across space and time. *Canadian Journal of Fisheries and Aquatic Sciences*, *64*(10), 1429–1447. https://doi.org/10.1139/F07-111

Maheu, A., Poff, N. L., & St-Hilaire, A. (2016). A classification of stream water temperature regimes in the conterminous USA. *River Research and Applications*, *32*(5), 896–906. https://doi.org/10.1002/rra.2906

Maitland, B. M., & Latzka, A. W. (2022). Shifting climate conditions affect recruitment in Midwestern stream trout, but depend on seasonal and spatial context. *Ecosphere*, *13*(12), e4308. https://doi.org/10.1002/ecs2.4308

McCluney, K. E., Poff, N. L., Palmer, M. A., Thorp, J. H., Poole, G. C., Williams, B. S., Williams, M. R., & Baron, J. S. (2014). Riverine macrosystems ecology: Sensitivity, resistance, and resilience of whole river basins with human alterations. *Frontiers in Ecology and the Environment*, *12*(1), 48–58. https://doi.org/10.1890/120367

McCullough, D. A., Bartholow, J. M., Jager, H. I., Beschta, R. L., Cheslak, E. F., Deas, M. L., Ebersole, J. L., Foott, J. S., Johnson, S. L., Marine, K. R., Mesa, M. G., Petersen, J. H., Souchon, Y., Tiffan, K. F., & Wurtsbaugh, W. A. (2009). Research in thermal biology: Burning questions for coldwater stream fishes. *Reviews in Fisheries Science*, *17*(1), 90–115. https://doi.org/10.1080/10641260802590152

McLaughlin, B. C., Ackerly, D. D., Klos, P. Z., Natali, J., Dawson, T. E., & Thompson, S. E. (2017). Hydrologic refugia, plants, and climate change. *Global Change Biology*, *23*(8), 2941–2961. https://doi.org/10.1111/gcb.13629

Meador, M. R. (2005). Single-pass versus two-pass boat electrofishing for characterizing river fish assemblages: Species richness estimates and sampling distance. *Transactions of the American Fisheries Society*, *134*(1), 59–67. https://doi.org/10.1577/FT03-094.1

Meisner, J. D. (1990). Effect of climatic warming on the southern margins of the native range of brook trout, Salvelinus fontinalis. *Canadian Journal of Fisheries and Aquatic Sciences*, *47*(6), 1065–1070. https://doi.org/10.1139/f90-122

Meyer, K. A., Lamansky, J. A., & Schill, D. J. (2006). Evaluation of an unsuccessful Brook Trout electrofishing removal project in a small Rocky Mountain stream. *North American Journal of Fisheries Management*, *26*(4), 849–860. https://doi.org/10.1577/M05-110.1

Michaletz, P. H., & Siepker, M. J. (2013). Trends and synchrony in Black Bass and Crappie recruitment in Missouri reservoirs. *Transactions of the American Fisheries Society*, *142*(1), 105–118. https://doi.org/10.1080/00028487.2012.722168

Midway, S. R., & Peoples, B. K. (2019). Effects of life-history traits on stream fish abundances across spatial scales. *Ecology of Freshwater Fish*, *28*(4), 639–649. https://doi.org/10.1111/eff.12482

Moran, P. A. P. (1953). The statistical analysis of the Canadian Lynx Cycle: II. Synchronization and meteorology. *Australian Journal of Zoology*, *1*(3), 291–298. https://doi.org/10.1071/ZO9530291

Morelli, T. L., Barrows, C. W., Ramirez, A. R., Cartwright, J. M., Ackerly, D. D., Eaves, T. D., Ebersole, J. L., Krawchuk, M. A., Letcher, B. H., Mahalovich, M. F., Meigs, G. W., Michalak, J. L., Millar, C. I., Quiñones, R. M., Stralberg, D., & Thorne, J. H. (2020). Climate-change

refugia: Biodiversity in the slow lane. *Frontiers in Ecology and the Environment*, *18*(5), 228–234. https://doi.org/10.1002/fee.2189

Myers, R. A., Mertz, G., & Bridson, J. (1997). Spatial scales of interannual recruitment variations of marine, anadromous, and freshwater fish. *Canadian Journal of Fisheries and Aquatic Sciences*, *54*(6), 1400–1407. https://doi.org/10.1139/f97-045

National Oceanic and Atmospheric Administration, National Centers for Environmental Information. (2022). *Climate Data Online*.

Nielsen, J. L. (1995). Evolution and the aquatic ecosystem: Defining unique units in population conservation. *American Fisheries Society Symposium. 1995.*

Ogle, D. H., Doll, J. C., Wheeler, P., & Dinno, A. (2022). *FSA: Fisheries Stock Analysis*.

Peterson, E. E., Merton, A. A., Theobald, D. M., & Urquhart, N. S. (2006). Patterns of spatial autocorrelation in stream water chemistry. *Environmental Monitoring and Assessment*, *121*(1), 571–596. https://doi.org/10.1007/s10661-005-9156-7

Poff, N. L., Allan, J. D., Bain, M. B., Karr, J. R., Prestegaard, K. L., Richter, B. D., Sparks, R. E., & Stromberg, J. C. (1997). The natural flow regime. *BioScience*, *47*(11), 769–784. https://doi.org/10.2307/1313099

Pörtner, H.-O., Roberts, D. C., Adams, H., Adler, C., Aldunce, P., Ali, E., Begum, R. A., Betts, R., Kerr, R. B., Biesbroek, R., et al. (2022). *Climate Change 2022: Impacts, Adaptation and Vulnerability. IPCC Sixth Assessment Report.* IPCC Geneva, The Netherlands.

Post, E., & Forchhammer, M. C. (2002). Synchronization of animal population dynamics by large-scale climate. *Nature*, *420*(6912), 168–171. https://doi.org/10.1038/nature01064

Pregler, K. C., Kanno, Y., Rankin, D., Coombs, J. A., & Whiteley, A. R. (2018). Characterizing genetic integrity of rear-edge trout populations in the southern Appalachians. *Conservation Genetics*, *19*(6), 1487–1503. https://doi.org/10.1007/s10592-018-1116-1

R Core Team. (2022). *R: A Language and Environment for Statistical Computing*. R Foundation for Statistical Computing.

Rahel, F. J., Keleher, C. J., & Anderson, J. L. (1996). Potential habitat loss and population fragmentation for cold water fish in the North Platte River drainage of the Rocky Mountains: Response to climate warming. *Limnology and Oceanography*, *41*(5), 1116–1123. https://doi.org/10.4319/lo.1996.41.5.1116

Ranta, E., Kaitala, V., Lindstrom, J., & Linden, H. (1995). Synchrony in population dynamics. *Proceedings of the Royal Society B: Biological Sciences*, *262*(1364), 113–118. https://doi.org/10.1098/rspb.1995.0184

Ranta, E., Lindstrom, J., Kaitala, V., Kokko, H., Linden, H., & Helle, E. (1997). Solar activity and hare dynamics: A cross-continental comparison. *The American Naturalist*, *149*(4), 765–775. https://doi.org/10.1086/286019

Reyjol, Y., Tedesco, P. A., & Lim, P. (2008). Stage-dependent spatial synchrony revealed for fish populations in the Garonne River (SW France). *Aquatic Sciences*, *70*(2), 179–185. https://doi.org/10.1007/s00027-008-8030-4

Rodríguez, M. A. (2002). Restricted movement in stream fish: The paradigm is incomplete, not lost. *Ecology*, *83*(1), 1–13. https://doi.org/10.1890/0012-9658(2002)083%5B0001:RMISFT%5D2.0.CO;2

Roghair, C. N., Dolloff, C. A., & Underwood, M. K. (2002). Response of a Brook Trout population and instream habitat to a catastrophic flood and debris flow. *Transactions of the American Fisheries Society*, *131*(4), 718–730. https://doi.org/10.1577/1548-8659(2002)131%3C0718:ROABTP%3E2.0.CO;2

Rosenberg, A., Bigford, T. E., Leathery, S., Hill, R. L., & Bickers, K. (2000). Ecosystem approaches to fishery management through essential fish habitat. *Bulletin of Marine Science*, *66*(3), 535–

542.

Roy, M., Holt, R. D., & Barfield, M. (2005). Temporal autocorrelation can enhance the persistence and abundance of metapopulations comprised of coupled sinks. *The American Naturalist*, *166*(2), 246–261. https://doi.org/10.1086/431286

Royama, T. (1992). Analytical population dynamics Chapman & Hall. *London, United Kingdom*.

Royle, J. A. (2004). N-mixture models for estimating population size from spatially replicated counts. *Biometrics*, *60*(1), 108–115. https://doi.org/10.1111/j.0006-341X.2004.00142.x

Saether, B.-E., Sutherland, W. J., & Engen, S. (2004). Climate Influences on Avian Population Dynamics. In *Advances in Ecological Research* (Vol. 35, pp. 185–209). Academic Press. https://doi.org/10.1016/S0065-2504(04)35009-9

Santiago, J. M., Muñoz-Mas, R., Solana-Gutiérrez, J., García de Jalón, D., Alonso, C., Martínez-Capel, F., Pórtoles, J., Monjo, R., & Ribalaygua, J. (2017). Waning habitats due to climate change: The effects of changes in streamflow and temperature at the rear edge of the distribution of a cold-water fish. *Hydrology and Earth System Sciences*, *21*(8), 4073–4101. https://doi.org/10.5194/hess-21-4073-2017

Schaub, M., & Kéry, M. (2012). Combining information in hierarchical models improves inferences in population ecology and demographic population analyses. *Animal Conservation*, *15*(2), 125–126. https://doi.org/10.1111/j.1469-1795.2012.00531.x

Schindler, D. E., Armstrong, J. B., & Reed, T. E. (2015). The portfolio concept in ecology and evolution. *Frontiers in Ecology and the Environment*, *13*(5), 257–263. https://doi.org/10.1890/140275

Schindler, D. E., Hilborn, R., Chasco, B., Boatright, C. P., Quinn, T. P., Rogers, L. A., & Webster, M. S. (2010). Population diversity and the portfolio effect in an exploited species. *Nature*, *465*(7298), 609–612. https://doi.org/10.1038/nature09060

Schlosser, I. J. (1985). Flow regime, juvenile abundance, and the assemblage structure of stream fishes. *Ecology*, *66*(5), 1484–1490. https://doi.org/10.2307/1938011

SDAFS Trout Committee. (1992). *Standardized Sampling Guidelines for Wadeable Trout Streams*.

Soranno, P. A., Cheruvelil, K. S., Bissell, E. G., Bremigan, M. T., Downing, J. A., Fergus, C. E., Filstrup, C. T., Henry, E. N., Lottig, N. R., Stanley, E. H., Stow, C. A., Tan, P.-N., Wagner, T., & Webster, K. E. (2014). Cross-scale interactions: Quantifying multi-scaled cause–effect relationships in macrosystems. *Frontiers in Ecology and the Environment*, *12*(1), 65–73. https://doi.org/10.1890/120366

Stenseth, N. C., Mysterud, A., Ottersen, G., Hurrell, J. W., Chan, K.-S., & Lima, M. (2002). Ecological effects of climate fluctuations. *Science*, *297*(5585), 1292–1296. https://doi.org/10.1126/science.1071281

Sutcliffe, O. L., Thomas, C. D., & Moss, D. (1996). Spatial synchrony and asynchrony in butterfly population dynamics. *Journal of Animal Ecology*, *65*(1), 85–95. https://doi.org/10.2307/5702

Sweka, J. A., & Wagner, T. (2022). Influence of seasonal extreme flows on Brook Trout recruitment. *Transactions of the American Fisheries Society*, *151*(2), 231–244. https://doi.org/10.1002/tafs.10347

Tedesco, P. A., Hugueny, B., Paugy, D., & Fermon, Y. (2004). Spatial synchrony in population dynamics of West African fishes: A demonstration of an intraspecific and interspecific Moran Effect. *Journal of Animal Ecology*, *73*(4), 693–705. https://doi.org/10.1111/j.0021-8790.2004.00843.x

Terui, A., Ishiyama, N., Urabe, H., Ono, S., Finlay, J. C., & Nakamura, F. (2018). Metapopulation stability in branching river networks. *Proceedings of the National Academy of Sciences*, *115*(26), E5963–E5969. https://doi.org/10.1073/pnas.1800060115

Thornton, P. E., Running, S. W., & White, M. A. (1997). Generating surfaces of daily meteorolog-

ical variables over large regions of complex terrain. *Journal of Hydrology*, *190*(3-4), 214–251. https://doi.org/10.1016/S0022-1694(96)03128-9

Thornton, P. E., Shrestha, R., Thornton, M., Kao, S. C., Wei, Y., & Wilson, B. E. (2021). Gridded daily weather data for North America with comprehensive uncertainty quantification. *Nature Publishing Group*, *8*(1), 1–17. https://doi.org/10.1038/s41597-021-00973-0

Thornton, P. E., Thornton, M. M., Mayer, B. W., Wilhelmi, N., Wei, Y., Devarakonda, R., & Cook, R. B. (2014). Daymet: Daily surface weather data on a 1-km grid for North America, Version 2. Data set. In *Oak Ridge National Laboratory Distributed Active Archive Center, Oak Ridge, Tennessee, USA*. https://doi.org/10.3334/ORNLDAAC/1840

U.S. Geological Survey. (2016). *NHDPlus Version 2*.

Vendrametto Granzotti, R., Agostinho, A. A., & Bini, L. M. (2022). Drivers and spatial patterns of population synchrony of fish species in a floodplain. *Freshwater Biology*, *67*(5), 857–872. https://doi.org/10.1111/fwb.13886

Waples, R. S. (1991). Pacific salmon, Oncorhynchus spp., And the definition of "species" under the Endangered Species Act. *Marine Fisheries Review*, *53*(3), 11–22.

Warren, D. R., Robinson, J. M., Josephson, D. C., Sheldon, D. R., & Kraft, C. E. (2012). Elevated summer temperatures delay spawning and reduce redd construction for resident brook trout (Salvelinus fontinalis). *Global Change Biology*, *18*(6), 1804–1811. https://doi.org/10.1111/j.1365-2486.2012.02670.x

Wehrly, K. E., Wang, L., & Mitro, M. (2007). Field-based estimates of thermal tolerance limits for trout: Incorporating exposure time and temperature fluctuation. *Transactions of the American Fisheries Society*, *136*(2), 365–374. https://doi.org/10.1577/t06-163.1

Wiens, J. A. (1989). Spatial scaling in ecology. *Functional Ecology*, *3*(4), 385–397. https://doi.org/10.2307/2389612

Wikle, C. K., Berliner, L. M., & Cressie, N. (1998). Hierarchical Bayesian space-time models. *Environmental and Ecological Statistics*, *5*(2), 117–154. https://doi.org/10.1023/A:1009662704779

Wilcox, K. R., Tredennick, A. T., Koerner, S. E., Grman, E., Hallett, L. M., Avolio, M. L., La Pierre, K. J., Houseman, G. R., Isbell, F., Johnson, D. S., Alatalo, J. M., Baldwin, A. H., Bork, E. W., Boughton, E. H., Bowman, W. D., Britton, A. J., Cahill Jr., J. F., Collins, S. L., Du, G., … Zhang, Y. (2017). Asynchrony among local communities stabilises ecosystem function of metacommunities. *Ecology Letters*, *20*(12), 1534–1545. https://doi.org/10.1111/ele.12861

Wohl, E. (2017). The significance of small streams. *Frontiers of Earth Science*, *11*(3), 447–456. https://doi.org/10.1007/s11707-017-0647-y

Xu, C. L., Letcher, B. H., & Nislow, K. H. (2010). Size-dependent survival of brook trout Salvelinus fontinalis in summer: Effects of water temperature and stream flow. *Journal of Fish Biology*, *76*(10), 2342–2369. https://doi.org/10.1111/j.1095-8649.2010.02619.x

Zorn, T. G., & Nuhfer, A. J. (2007). Influences on Brown Trout and Brook Trout population dynamics in a Michigan river. *Transactions of the American Fisheries Society*, *136*(3), 691–705. https://doi.org/10.1577/T06-032.1

APPENDIX

Table S1: Data availability by agency. 'Years Data' indicates temporal coverage within the data range.

Agency	Date Range	Years Data
GA Dept. Natural Resources	1982 - 2014	16
Shenandoah Nat'l Park	2011 - 1997	31
VA Dept. Wildlife Resources	1982 - 1999	18
TN Wildlife Resources Agency	1982 - 2014	15
US Geological Survey	1982 - 2009	23
MD Dept. Natural Resources	1982 - 2007	27
Great Smoky Mountain Nat'l Park	1982 - 2015	28
Clemson Univ.	1982 - 2003	16
NC Wildlife Resources Commission	1982 - 1990	11

Simulation for Missing Data in Correlogram Analysis

A simulation study was undertaken to evaluate the feasibility of interpreting correlograms created using a dataset with a large percentage of imputed values for missing data. Due to irregular sampling by managers and limited multipass electrofishing data, the time series of yearly brook trout densities was missing 47% of values. We chose to impute these missing values with the mean density in the given segment during the 20 year time period of interest (1995-2015). Here, we simulate spatially-autocorrelated datasets with 0%, 25%, 50%, and 75% missing data, comparing the resulting correlograms.

```
set.seed(1234)

### Simulate 0 pct missingness data at 100 sites
### over 2 years
x <- expand.grid(1:20, 1:5)[, 1]
y <- expand.grid(1:20, 1:5)[, 2]
# true range (p) is 2 under Gaussian covariance
# function
Z <- cbind(rmvn.spa(x = x, y = y, p = 2, method = "gaus"),
    rmvn.spa(x = x, y = y, p = 2, method = "gaus"))
# Fit correlogram
fit0 <- Sncf(x = x, y = y, z = Z, resamp = 1000, quiet = T)
plot0 <- ~plot(fit0)
m0.summary <- summary(fit0)

### 25 pct missingness
Z.m25 <- Z
Z.m25[sample(length(x), 0.25 * length(x))] <- NA
for (i in 1:nrow(Z)) {
    idx.tmp <- which(is.na(Z.m25[i, ]))
    if (length(idx.tmp > 0)) {
        Z.m25[i, idx.tmp] <- mean(Z.m25[i, ], na.rm = TRUE)
    }
}
# Fit correlogram
fit25 <- Sncf(x = x, y = y, z = Z.m25, resamp = 1000,
    quiet = T)
plot25 <- ~plot(fit25)
m25.summary <- summary(fit25)

### 50 pct missingness
Z.m50 <- Z
Z.m50[sample(length(x), 0.5 * length(x))] <- NA
for (i in 1:nrow(Z)) {
    idx.tmp <- which(is.na(Z.m50[i, ]))
    if (length(idx.tmp > 0)) {
        Z.m50[i, idx.tmp] <- mean(Z.m50[i, ], na.rm = TRUE)
    }
```

```
}
# Fit correlogram
fit50 <- Sncf(x = x, y = y, z = Z.m50, resamp = 1000,
    quiet = T)
plot50 <- ~plot(fit50)
m50.summary <- summary(fit50)

### 75 pct missingness
Z.m75 <- Z
Z.m75[sample(length(x), 0.75 * length(x))] <- NA
for (i in 1:nrow(Z)) {
    idx.tmp <- which(is.na(Z.m75[i, ]))
    if (length(idx.tmp > 0)) {
        Z.m75[i, idx.tmp] <- mean(Z.m75[i, ], na.rm = TRUE)
    }
}
# Fit correlogram
fit75 <- Sncf(x = x, y = y, z = Z.m75, resamp = 1000,
    quiet = T)
plot75 <- ~plot(fit75)
m75.summary <- summary(fit75)

## Make a compound plot
SimStudy_compound.plot <- plot_grid(plot0, plot25,
    plot50, plot75, labels = c("a)", "b)", "c)", "d)"))
```

Comparing the four simulations, we see that the 95% confidence interval grows when increasing amounts of missing data are imputed with means. Mean pairwise correlation estimates do not significantly differ between the first three simulations (0%: 0.31, (0.14, 0.51), 25%: 0.29, (0.11, 0.52), 50%: 0.26, (0.03, 0.53)). Neither do estimates of the distance at which pairwise correlation reaches 0 (0%: 14.13, (8.85, 16.16), 25%: 13.1, (8.37, 15.74), 50%: 15.19, (2.9, 17.13)). We take this as evidence that imputing 47% missing data with site mean density does not considerably effect interpretations of the magnitude or scale of spatial synchrony.

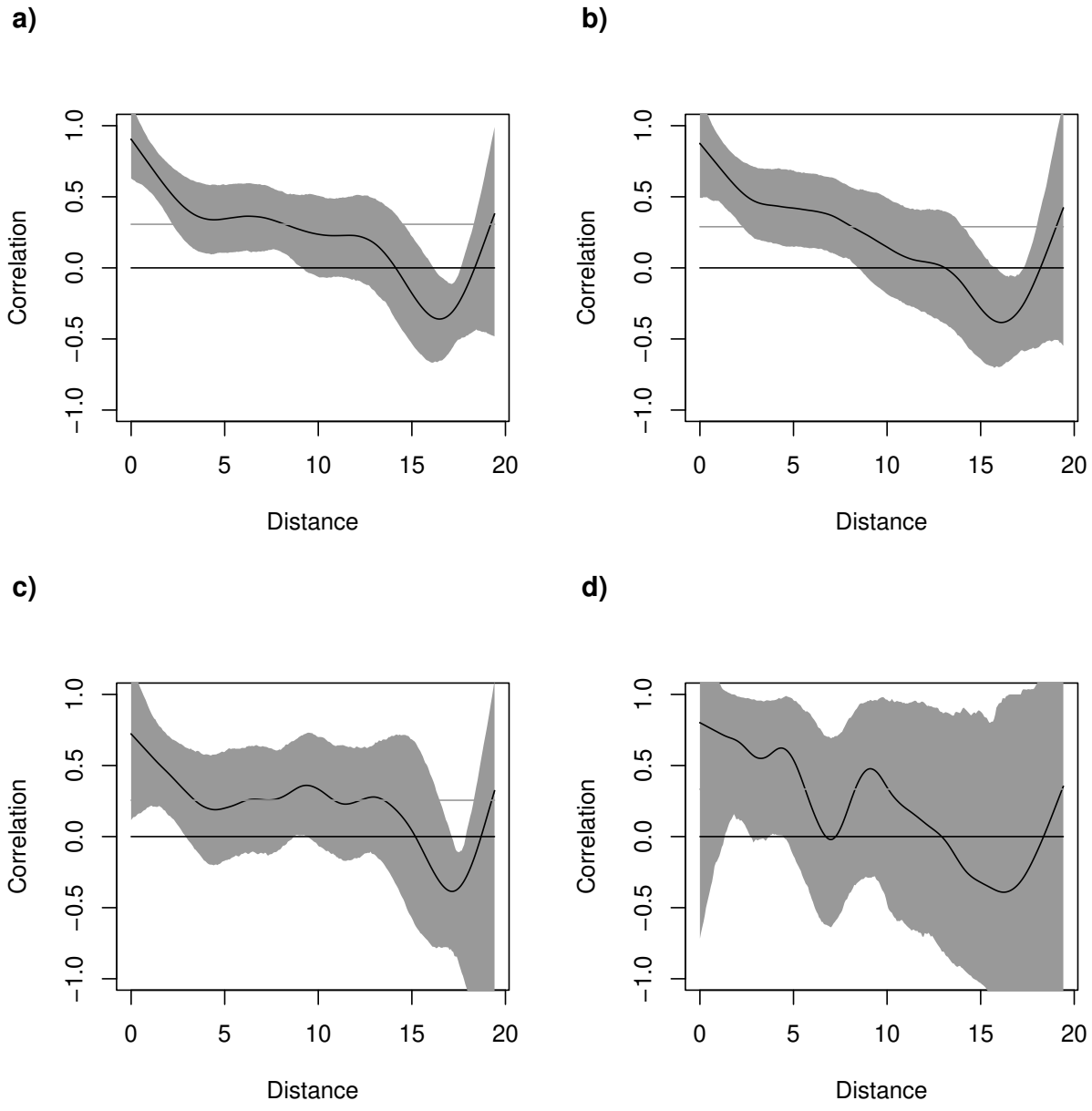

Figure S1: Spline correlogram of a datasets with a) 0%, b) 25%, c) 50%, and d) 75% missingness over 2 years at 100 sites. Grey shading represents 95% confidence interval. Grey line represents mean correlation.

Simulation for Combined Model

We developed a simulation to evaluate the identifiability of a model with both climate effects and random effects. We simulated 3-pass electrofishing data for 100 stream segments over 20 years, and evaluated with an an N-mixture model using a removal mechanism coupled with a log linear process model. We simulated one spatially heterogeneous climate covariate and both temporal and spatiotemporal random effects. Detection probability was the same for all simulated stream segments.

```
set.seed(1234)

## settings
nSites <- 100
nYears <- 20
nPasses <- 3
# climate cov (mean standardized):
x <- matrix(rnorm(nSites * nYears), nrow = nSites,
    ncol = nYears)
# site specific intercept:
alpha0 <- runif(nSites, min = 3, max = 4.5)
# spatially heterogeneous climate cov effect:
alpha1 <- rnorm(nSites, mean = -0.3, sd = 0.3)
# time random effect:
eps <- rnorm(nYears, mean = 0, sd = 0.4)
# time-site random effect:
gamma <- matrix(rnorm(nSites * nYears, mean = 0, sd = 0.2),
    nrow = nSites, ncol = nYears)
p <- 0.6  # capture prob per pass
N <- lam <- array(dim = c(nSites, nYears))
y <- array(dim = c(nSites, nYears, nPasses))

## simulate abundance
for (i in 1:nSites) {
    for (t in 1:nYears) {
        lam[i, t] <- exp(alpha0[i] + alpha1[i] * x[i,
            t] + eps[t] + gamma[i, t])
        N[i, t] <- rpois(1, lam[i, t])
    }
}

## simulate data
for (i in 1:nSites) {
    for (t in 1:nYears) {
        y[i, t, 1] <- rbinom(1, N[i, t], p)
        y[i, t, 2] <- rbinom(1, N[i, t] - y[i, t, 1],
            p)
        y[i, t, 3] <- rbinom(1, N[i, t] - y[i, t, 1] -
            y[i, t, 2], p)
```

```
    }
}


# Bundle data
jags_data <- list(nSites = nSites, nYears = nYears,
    x = x, y = y)


# Parameters to save
jags_params <- c("omega", "beta", "mu.beta", "s2.beta",
    "sd.beta", "p", "sd.eps", "s2.eps", "sd.gam", "s2.gam")

# Create and populate an array of initial values
# for N.YOY.  Initial values must all be great
# than or equal to the sum of observed counts
N.inits <- array(numeric(), dim = c(nSites, nYears))
for (i in 1:nSites) {
    for (t in 1:nYears) {
        N.inits[i, t] <- round(as.numeric(ifelse(is.na((y[i,
            t, 1] + y[i, t, 2] + y[i, t, 3])), rpois(1,
            lambda = 200), (y[i, t, 1] + y[i, t, 2] +
            y[i, t, 3] + 1) * 2)))
    }
}

# Set initial values
init_vals <- function() list(omega = runif(nSites,
    0, 5), sd.beta = runif(1, 0, 10), mu.beta = rnorm(1,
    -0.5, 0.01), p = 0.6, N = N.inits)


# MCMC settings
ni <- 20000
nc <- 3
nb <- 5000
nt <- 1


# Fit Model
nMix_sim <- jagsUI::jags(data = jags_data, parameters.to.save = jags_params,
    model.file = here("Analysis/nMix_JAGS_files", "nMix_sim.jags"),
    n.chains = nc, n.iter = ni, n.burnin = nb, n.thin = nt,
    parallel = T, inits = init_vals)

# What proportion of the sd.gams include the true
# value (0.2) in their 95% HPDI?
```

```r
nMix_sim_sd.gams <- MCMCsummary(nMix_sim, params = "sd.gam",
    HPD = T) %>%
    mutate(cont_true = ifelse((0.2 >= .[, 3] & 0.2 <=
        .[, 4]), TRUE, FALSE))

nrow(nMix_sim_sd.gams[nMix_sim_sd.gams$cont_true ==
    TRUE, ])/nrow(nMix_sim_sd.gams) * 100

# Plot posteriors of estimated values vs original
# values
sim_plot_data <- data.frame(sample_val = rbind(as.matrix(nMix_sim$sims.list$mu.beta),
    as.matrix(nMix_sim$sims.list$sd.beta), as.matrix(nMix_sim$sims.list$sd.eps),
    as.matrix(nMix_sim$sims.list$sd.gam[, 1]), as.matrix(nMix_sim$sims.list$p)),
    parameter = rep(c("mu.beta", "sd.beta", "sd.eps",
        "sd.gam", "p"), each = length(nMix_sim$sims.list$mu.beta)))

# specify order of the parameters to plot
sim_plot_data$parameter <- factor(sim_plot_data$parameter,
    c("mu.beta", "sd.beta", "sd.eps", "sd.gam", "p"))

# these are the generating values for the dataset
hlines <- data.frame(y = c(-0.3, 0.3, 0.4, 0.2, 0.6),
    x = c(1, 2, 3, 4, 5))

CombinedModel_Sim.plot <- ggplot() + geom_violin(data = sim_plot_data,
    aes(x = parameter, y = sample_val), scale = "width") +
    geom_segment(data = hlines, aes(x = x - 0.5, xend = x +
        0.5, y = y, yend = y), color = "red", size = 0.8,
        linetype = "dashed") + labs(x = "Parameter",
    y = "Value") + theme_classic()

CombinedModel_Sim.plot
```

Code

Code can be found online at github.com/gpvalentine/SE_Trout.

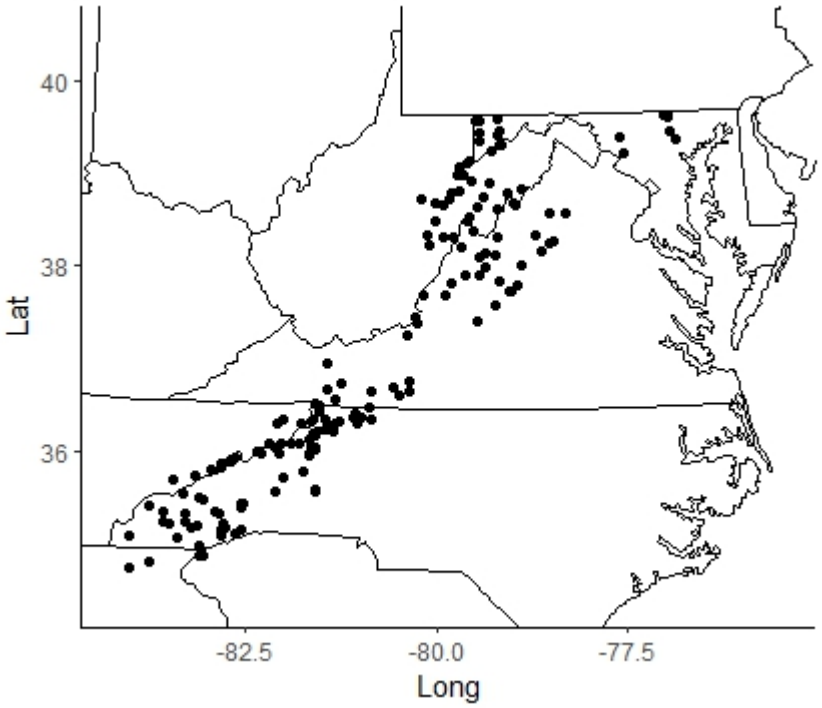

Figure S2: Locations of 204 paired air and water temperature sensors. Sites were located in randomly selected subwatersheds identified as capable of supporting populations of brook trout (*Salvelinus fontinalis*, Eastern Brook Trout Joint Venture, 2006). Located at the downstream outlet of the subwatersheds, at each site a logger underwater was paired with a logger affixed to the bank or a tree. Stream and air temperatures were measured every 30 minutes using remote loggers (Onset Computer Corporation, Bourne, MA 02532). Loggers were deployed from 2011 to 2015. Source: USDA Forest Service.

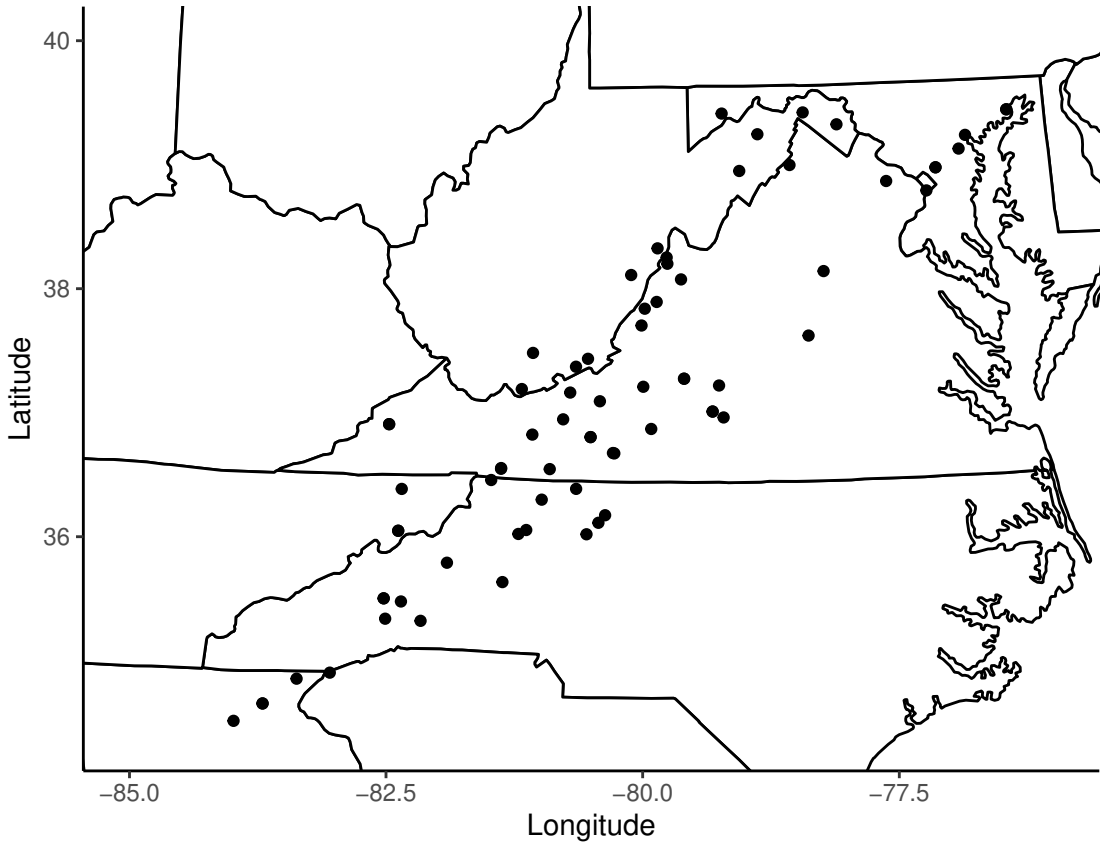

Figure S3: Locations of 51 stations within the study area where hourly precipitation data were measured. Source: NOAA NCEI

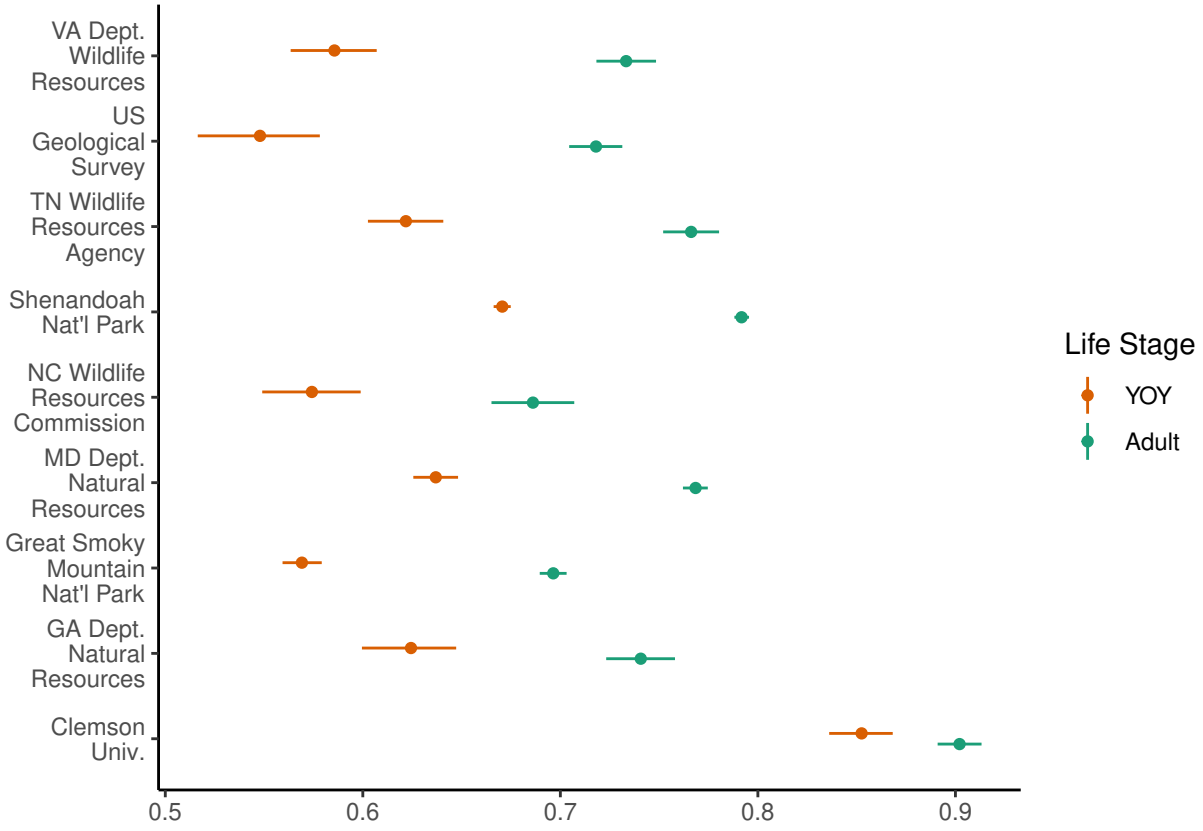

Figure S4: Per-pass electrofishing capture probability by data source. A combination of single- and multi-pass sampling methods (single: 29.9%, multi: 70.1%) were employed following standardized sampling protocols for the southern US region (SDAFS Trout Committee, 1992). In multi-pass sampling, fish were removed from the stream in successive passes in temporarily blocked stream reaches to estimate capture probability and thus population size. Sampling boundaries were defined by block nets or cobble dams which serve as barriers for fish movement. Depending on stream width, one to three backpack electrofishing units were used.

Table S2: Top ten correlations between climate covariates and local habitat. Correlations were tested for 182 segment, catchment, and watershed characteristics accessed from the USGS NHDplus and EPA StreamCat database. Abbreviations (descriptions from sources): VE_09 = Velocity for predicted runoff (September), PctCrop2016Cat = Percent of catchment area classified as crop land use (2016 NLCD class 82), VC_08 = Velocity for predicted runoff (August), VA_10 = Velocity for annual runoff (October), VA_09 = Velocity for annual runoff (September), VC_10 = Velocity for predicted runoff (October), VC_07 = Velocity for predicted runoff (July), QC_09 = Estimated flow (September), PctHay2016Ws = Percent of watershed classified as hay land use (2016 NLCD class 81), Pathlength = Distance downstream to network end (km).

Climate Covariate (\beta_i)	Local Habitat Variable	Spearman Correlation
Spring Flow	PctCrop2016Ws	-0.3030661
Spring Flow	VC_09	0.2839436
Summer Temperature	Winter Flow	-0.2802658
Winter Flow	Summer Temperature	-0.2802658
Spring Flow	PctHay2016Cat	-0.2789562
Winter Flow	DnHydroseq	0.2754755
Spring Flow	VE_09	0.2734770
Spring Flow	PctCrop2016Cat	-0.2706128
Spring Flow	VC_08	0.2652018
Spring Flow	VA_10	0.2634857

Table S3: Top ten correlations between YOY intraclass correlation coefficients (ICCs) and local habitat. Correlations were tested for 182 segment, catchment, and watershed characteristics accessed from the USGS NHDplus and EPA StreamCat database. Abbreviations (descriptions from sources): PctShrb2016Cat = Percent of catchment classified as shrub/scrub land cover (2016 NLCD class 52), PctShrb2016Ws = Percent of watershed classified as shrub/scrub land cover (2016 NLCD class 52), OmCat = Mean organic matter content (% by weight) of soils (STATSGO) within catchment, OmWs = Mean organic matter content (% by weight) of soils (STATSGO) within watershed, QC_02 = Adjusted predicted runoff (February), PctNonAgIntrodManagVegWs = % Nonagriculture nonnative introduced or managed vegetation landcover type reclassed from LANDFIRE Existing Vegetation Type (EVT), within watershed, VC_01 = Velocity for adjusted predicted runoff (January), VC_02 = Velocity for adjusted predicted runoff (February), BFIWs = % of baseflow (groundwater discharge) to total flow, within watershed, QE_02 = Gauge flow (February).

Local Habitat Variable	Spearman Correlation
PctShrb2016Cat	0.4117433
PctShrb2016Ws	0.3735396
ToNode	0.3222213
FromNode	0.3107517
OmCat	0.2922116
LevelPathI	0.2729284
DnLevelPat	0.2557286
TerminalPa	0.2550670
OmWs	0.2534310
QC_02	-0.2524774

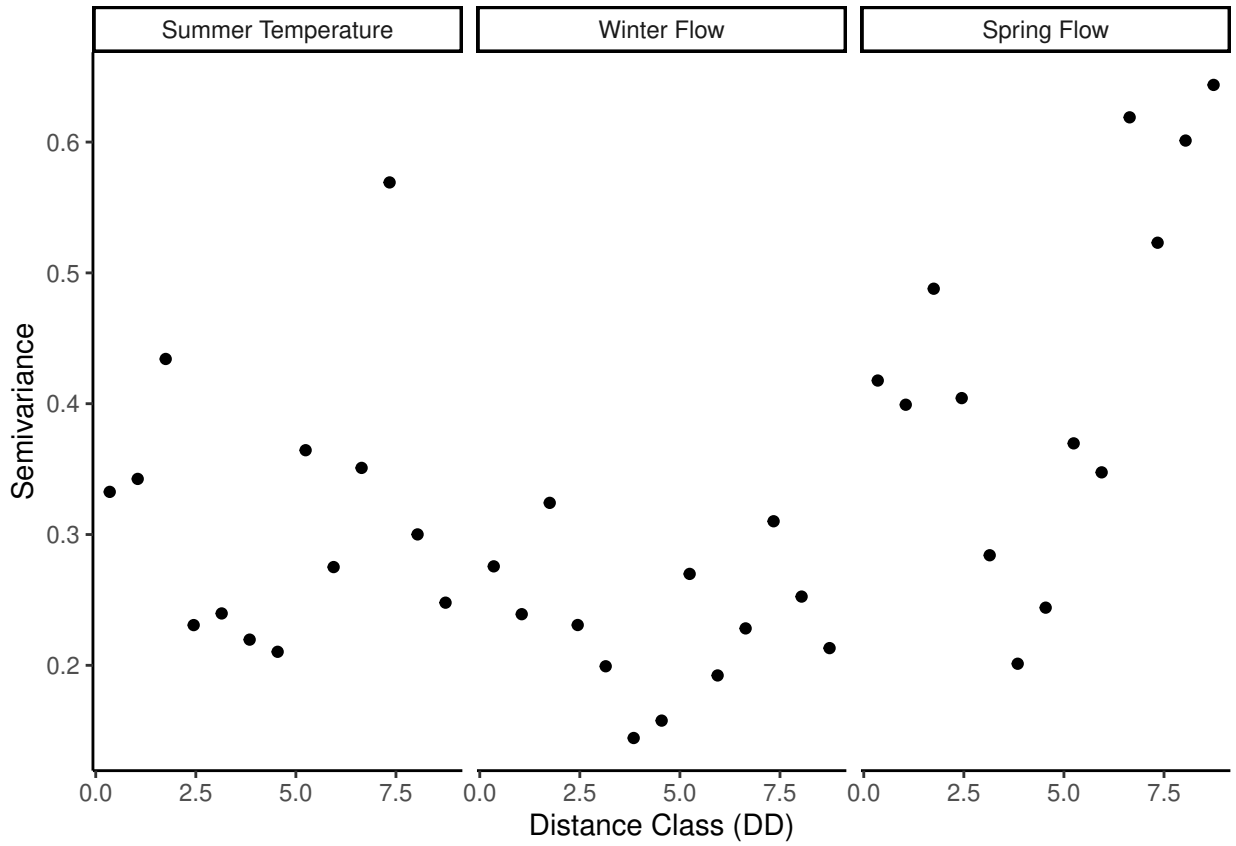

Figure S5: Semivariogram depicting spatial structure in stream segment-specific climate effects on abundance of young-of-year brook trout (*Salvelinus fontinalis*). If spatial structure is present, nearer values will have lover semivariance than farther values. Climate variables include: average 0.9Q summer air temperature (year t-1), max 0.9Q winter stream flow (year t), and max 0.9Q spring stream flow (year t). DD = Decimal degrees.

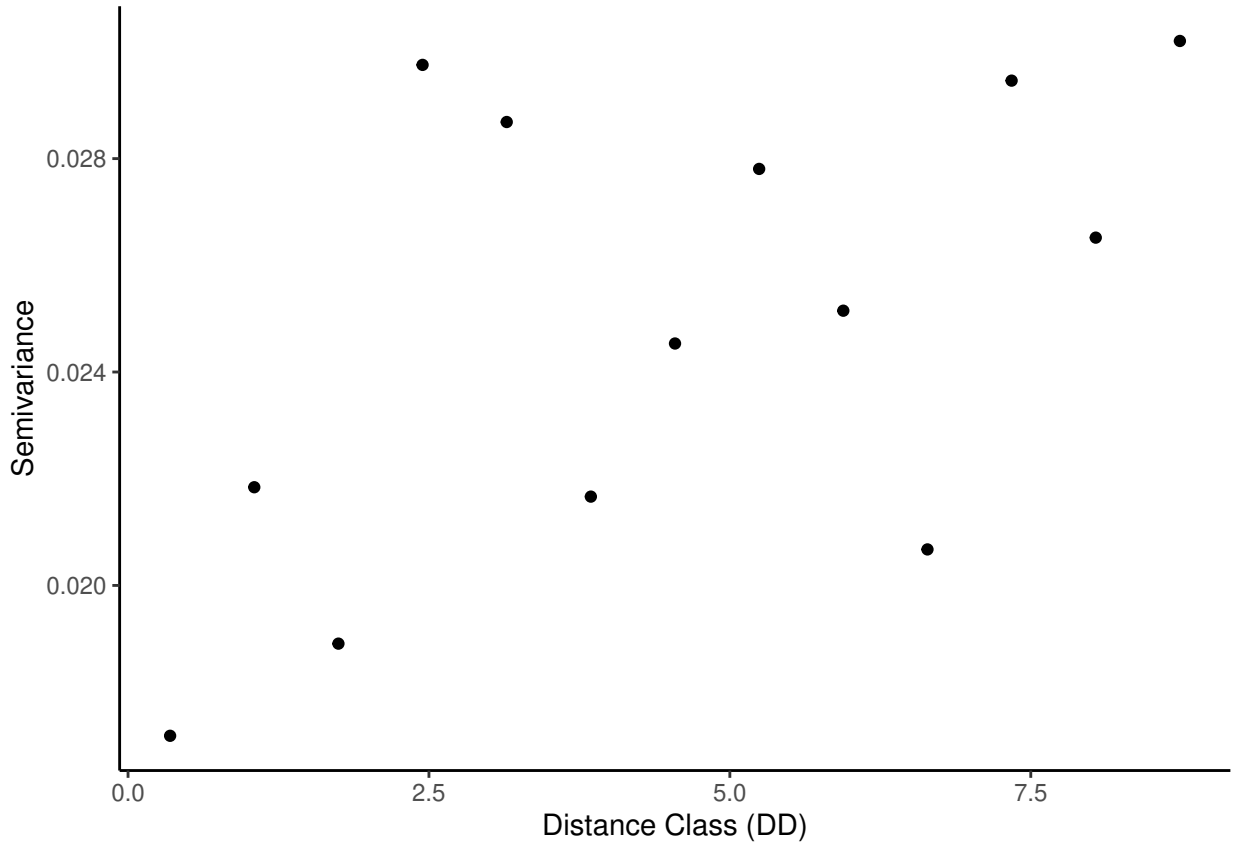

Figure S6: Semivariogram depicting spatial structure in stream segment-specific intraclass correlation coefficients (ICCs) of abundance of young-of-year brook trout (*Salvelinus fontinalis*). If spatial structure is present, nearer values will have lower semivariance than farther values. DD = Decimal degrees.

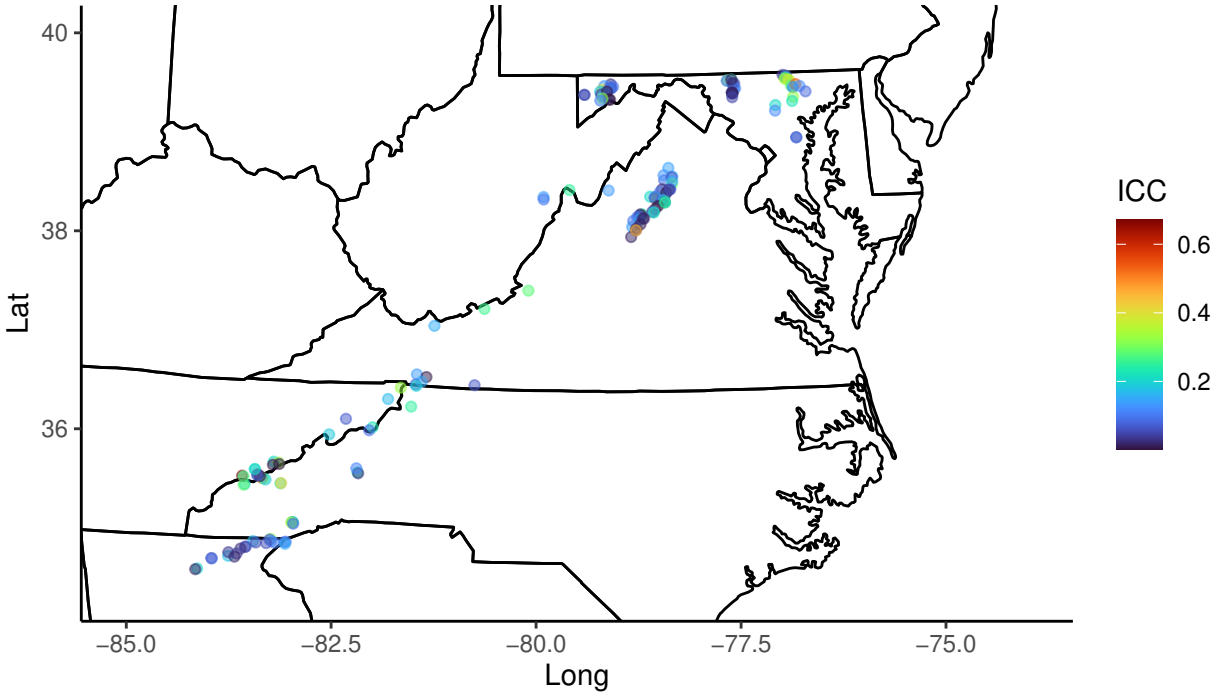

Figure S7: Intraclass correlation coefficient (ICC) values for populations of adult brook trout (*Salvelinus fontinalis*) in the southeastern USA. High ICC values indicate synchrony relative to the temporal variation averaged across segments, while low ICC values indicate asynchrony.

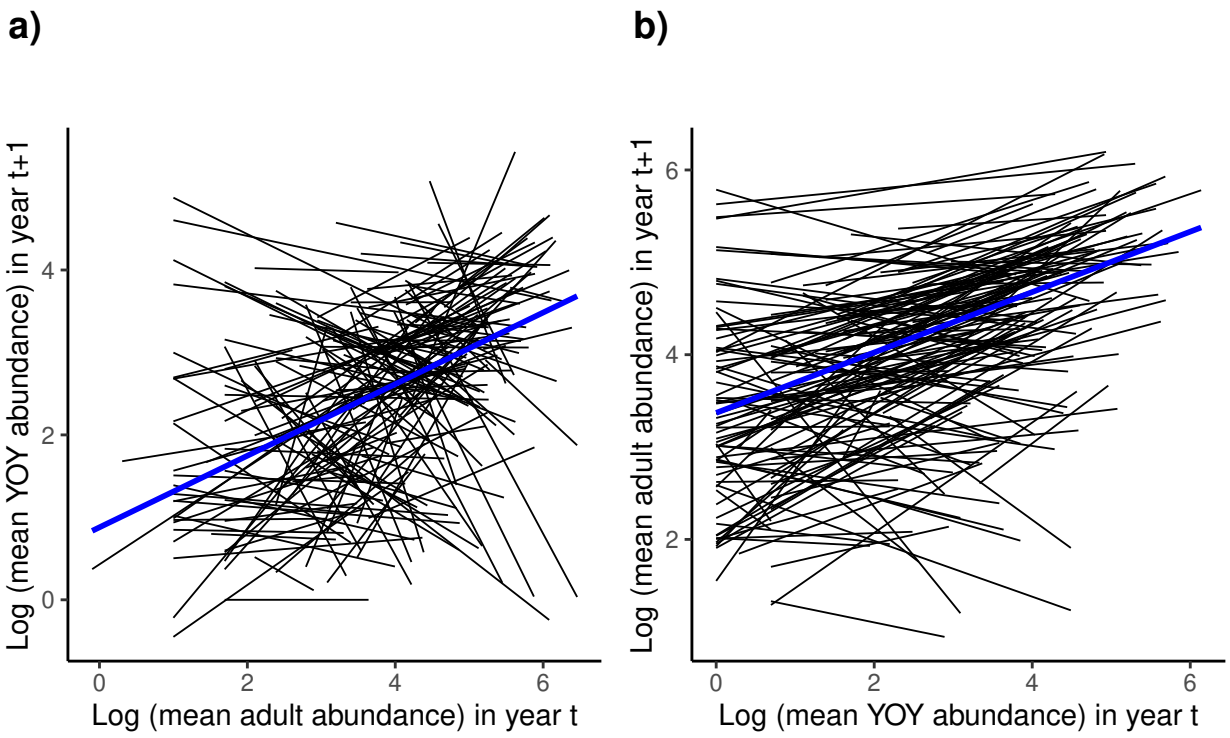

Figure S8: a) Stock-recruitment and b) recruitment-stock relationships for young-of-the-year (YOY) and adult brook trout (*Salvelinus fontinalis*) in the 170 stream segments considered in the present analysis. Black lines represent stream segment-specific relationships, and blue lines represent averaged relationships.

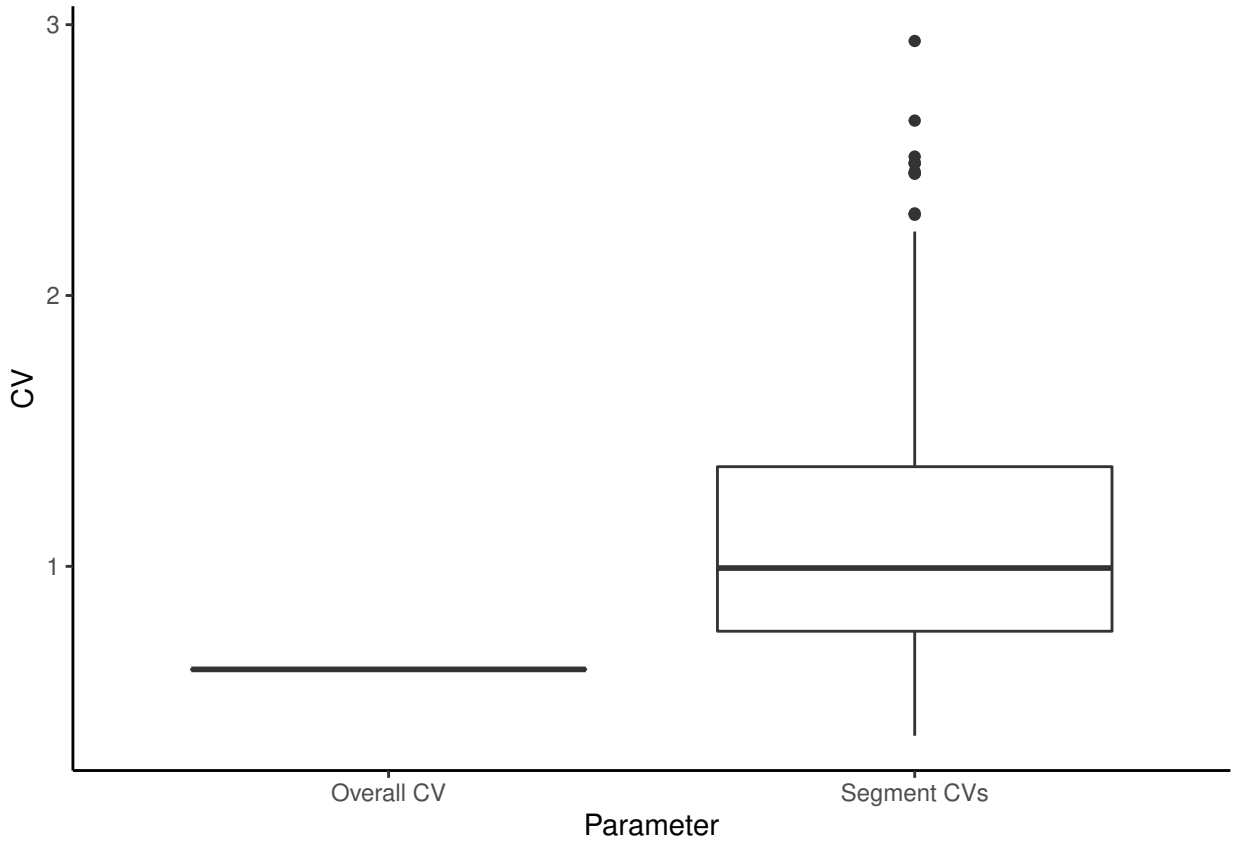

Figure S9: Overall and stream segment-specific coefficients of variation (CV) in observed pass 1 abundance of young-of-the-year brook trout (*Salvelinus fontinalis*). The dark black line represents the median, black box the interquartile range, and the whiskers the lowest/highest values within 1.5 times the interquartile range. Outliers beyond that range are represented by black dots.